

NATIONAL RADIO ASTRONOMY OBSERVATORY

Charlottesville, Virginia

Engineering Division Internal Report No. 110

The Design of the Deformable Subreflector  
for the 140 ft. Radio Telescope

W-Y. Wong

January, 1979

Number of copies: 100

The Design of a Deformable Subreflector for  
the 140-ft. Radio Telescope

W-Y. Wong

TABLE OF CONTENTS

	Page
I. SUMMARY . . . . .	1
II. THE SUBREFLECTOR . . . . .	2
General Description . . . . .	2
Geometry . . . . .	3
Material . . . . .	5
Stress Analyses . . . . .	6
Error Budget . . . . .	7
Deforming the Subreflector Surface . . . . .	9
The Motion of the Ideal Actuators . . . . .	10
Evaluations and Measurements of the Subreflector Surface . . . . .	11
Evaluationd and Measurements of the Experimental Actuators . . . . .	12
The Motion of the Experimental Actuators . . . . .	13
III. DEFORMING SYSTEM . . . . .	15
General Description . . . . .	15
Electronic Control . . . . .	15
Force Requirements on Actuators . . . . .	17
Type of Experimental Actuators . . . . .	18
The Linkage . . . . .	19
The Switching Off of the Actuator . . . . .	19

## TABLE OF CONTENTS

(Continued)

	Page
IV. BACK UP FRAME . . . . .	20
General Description . . . . .	20
The Design . . . . .	20
V. SOFTWARE PROGRAMMING . . . . .	22
General Description . . . . .	22
The Input and the Output . . . . .	22
VI. MEASURING JIG. . . . .	24
ACKNOWLEDGEMENT . . . . .	25
REFERENCE . . . . .	26
LIST OF TABLE . . . . .	28
FIGURE CAPTIONS . . . . .	33

## APPENDIX

A. Engineering Drawings of the Subreflector Surface . . . . .	40
B. Engineering Drawings of the Back up Frame. . . . .	48
C. Engineering Drawings of the Deforming System . . . . .	58
D. Engineering Drawings of the Measuring Jig. . . . .	63
E. Best Fit of a Hyperboloid. . . . .	70

## I. SUMMARY

It was suggested that the strong gravitational astigmatism of large radio telescopes can be corrected for by a shaped subreflector [1], if the error profile of the main reflector is reproduced at the subreflector and the reflecting rays do not cross each other [2]. Experiments by Cowles and Parker, using a 0.3m shaped subreflector on a 2.8m reflector show that the aperture efficiency was improved by a factor of two at 34 GHz [3]. The gravitational astigmatism of the 140 ft telescope was first indicated by structural analyses, and subsequently verified by S. Von Hoerner, using an elongated feed horn [4]. A 3.2m subreflector was built, with the profile mechanically deformed and electronically controlled. The amount of deformation varies with the telescope pointing.

This second subreflector includes all the features of the first subreflector: it is asymmetrical and tilttable. This report describes the detailed mechanical design, and ground level evaluation, of the subreflector. The electronic aspect of this subreflector: design of controller and the interface to the computer, is described in a separate report by R. Lacasse [5]. The test on the telescope with seven unresolved radio sources at 22.3 GHz gives considerable amount of improvements, especially far south and east. The best result shows the aperture efficiency was increased by a factor between two and three [6].

## II. THE SUBREFLECTOR

### General Description

The deformable subreflector has to follow the criteria that 1) the subreflector is asymmetrical due to the off-set feed arrangement; 2) the subreflector is tilttable for beam switching technique in observation; and 3) the subreflector is deformable to correct the gravitational astigmatism.

The first consideration was entirely geometric, readily defined when the first subreflector was implemented to the telescope system. The second consideration means that the weight and the moment of inertia of the new system has to be kept equal to, if not less than, the previous system. For the load capacity of the sterling mount, nominally set to 2500 lbs., was already exceeded. The third consideration was new to the system. Four servo controlled motor-actuators are installed at four points behind the subreflector. The amount of actuation is determined by the elevation position of the telescope.

The fiberglass, aluminum honeycomb core sandwich construction method is proven acceptable, in terms of cost and surface accuracy, by the first subreflector. The force required for the deformation of the surface, solved analytically, was found reasonable. Hence the same material and fabrication approach for the new surface was adopted. The long term behavior of this composite material is not entirely known, however. Aging, temperature, environment and cyclic loading effects might degrade the surface accuracy and reduce its usable life time. The surface of the first subreflector has degraded from the original error of 0.25 mm rms to 0.43 mm rms after four years.

The stiffening rib arrangement of these two subreflectors are also different. The first subreflector has a stiffening ring, whereas the second

one has two stiff diagonals. For both cases, however, the main structural stiffness is derived from the back-up frame which serves as an interface between the beam-tilt system and the subreflector surface.

Due to the off-set receiver arrangement, the deforming feature is applicable only to the feed position of the K-band maser receiver (22.3 GHz,  $\lambda = 1.23$  cm) plus three others, rotated by  $90^\circ$ . For other receiver positions, the subreflector's profile must be returned to its undeformed position.

The subreflector system can be dismounted from the telescope so that the optic of the system can be modified within a reasonably short period of time.

The front face of the subreflector is coated with a thin layer of aluminum film for reflection. The subreflector is painted white. The back-up frame is unpainted. All moving parts of the deforming system are protected by water-tight covers.

#### Geometry

A schematic arrangement of the Cassegrain system for the 140-ft telescope is shown in Figure 1. Some important parameters are given in the following list, describing the Cassegrain optics:

Average subreflector diameter = 3.213m (126.4")

Distance from the prime focus to secondary focus:  $a = 13.48\text{m}$   
(530.89")

Distance from the prime focus to subreflector vertex:

$$b = 1.30^{\text{m}} (51.262")$$

Magnification:  $m = 9.348$

Eccentricity:  $e = 1.240$

Angle between parabolic axis and hyperbolic axis:  $4.148^\circ$

The hyperboloid is given in eq. (1), describing the profile of the subreflector in an untilted system, with Z-axis as the hyperbolic axis.

$$z = \left(c - \frac{1}{2}a\right) \left\{ \sqrt{1 + \frac{r^2}{bc}} - 1 \right\} \quad (1)$$

where  $r^2 = x^2 + y^2$  and  $c = a-b$ .

The hyperbolic axis and the parabolic axis do not coincide. They subtend an angle of  $4.148^\circ$ . A cluster of feeds are arranged in a ring with a radius of 0.98m (38.58") and they are 4.57m (180") above the vertex [7]. The subreflectors' axis is aligned with the phase center of the feed in use by rotating the subreflector about the axis of the main reflector at the Sterling mount. The rim of the subreflector, which is the intersection of the hyperboloid and the cone defined by the line of sight of the prime system, is not a circle. The coordinates of the rim were computed by P. J. Napier and are listed in Table I for reference.

The rim is marked at every  $15^\circ$  with respect to the hyperbolic axis. A collimating mirror with cross-hair defines the hyperbolic axis. Another cross is marked 94.3 mm (1.714 in) from the hyperbolic axis along the plane of symmetry which defines the parabolic axis of the subreflector.

The arrangement of the actuators (A1 - A4) and the stationary connections (S1-S4) are also illustrated in Figure 1, showing their positions relative to the main reflector. The direction of the beam tilting is perpendicular to the parabolic and hyperbolic axes. The relative position of the subreflector to the main reflector is defined when a particular receiver is used. For example, the actuator A1 is aligned to the northern rim of the main reflector only when the K-band maser receiver is in use.

Material

The subreflector shell structure is composed of fiberglass cloths, and an aluminum honeycomb core. This sandwich construction is bonded together by epoxy resin cured by hardener, or curing agent. There are three plies of fiberglass cloth laminates on the front and the back of the shell. The thickness of each ply is 0.28mm (0.011 in). The honeycomb core is 25.4mm (1.0 in) thick.

The shell structure is laid out in steps in a mold and bonded together with the epoxy. The curing takes place inside the mold. Suction was constantly applied between the mold and the front surface to insure the reproduction of the profile in the mold. The curing agent was selected so that room temperature curing is adequate to achieve the necessary material strength. Shrinkage of the curing agent is claimed to be less than 2%.

A thin layer (about 0.15mm) of aluminum film was flame-sprayed onto the mold before the epoxy-fiberglass was applied to make the surface reflective.

The quality of this composite construction depends on the material properties of the components as well as on the skill of the fabrication, the type of curing agent and the duration of the curing. Temperature, pressure and types of fiberglass cloth also affect the strength of the product. Moreover, there is a wide selection of size, foil thickness and alloy of the aluminum honeycomb core. Because of the many possible combinations, the material properties of the final product is best determined by direct measurements. On the other hand, tests on specimens are usually

made by the manufacturer only when a large quantity of the product is involved. There were no such measurements made for this subreflector. The material properties used during the analyses are based on the best available data provided by the manufacturer. The results of the calculations should be considered good within 20%. The components of the subreflector are listed in Table II. The Antenna System Incorporated of San Jose, California, was responsible for the construction of the shell structure.

#### Stress Analyses

The in-house feasibility studies started in 1975, determining the actuator arrangement and basic stiffening geometry. The studies also provided a prediction on the improvement of the telescope surface error due to the astigmatic correction. All detail computations are filed in reference [8].

The final analysis was done by an outside firm - Control Data Corporation. The CDC computations [9] used an accurate mathematical model of the shell structure, with the geometry, material properties and loading conditions specified by N.R.A.O. The model has 180 finite elements and 108 nodes (Figure 2), made in one quadrant by assuming the subreflector is symmetrical. The model is constrained at node 57, and actuated at nodes 52 and 62. The four loading conditions considered in the analyses are:

- 1) Astigmatic deformation: node 52 and 62 were actuated in opposite directions by an amount of 1.57mm (0.062 in.);

- 2) Survival load: mode 52 and 62 were actuated in the same direction by 3.8mm (0.150 in.);
- 3) Acceleration due to tilting: the angular acceleration is  $34.4 \text{ rad/sec}^2$ , equivalent to the tilting of the subreflector at  $\lambda = 2\text{cm}$  observation, and
- 4) Thermal load of  $10^\circ\text{F}$  difference between the front and the back faces of the subreflector.

The analytical results are summarized in Table III. The large safety margin in the survival condition shows that the subreflector will survive an erroneous actuation, when all actuators actuate in the same direction. This mode of actuation is in fact a higher order astigmatic correction suggested in ref. [9], but presently not possible to produce.

The stiffness at the point of actuation are:

$$\left. \begin{array}{l} \text{1st mode astigmatic correction} = 201 \text{ N/mm} \\ \text{2nd mode astigmatic correction} = 417 \text{ N/mm} \end{array} \right\} \quad (2)$$

The accuracy of the analyses was proven to be good. Figure 3 shows a comparison of the measured and the computed profiles. When the subreflector is actuated by 1.57mm, the difference of these two profiles is 0.14 mm rms.

#### Error Budget

The surface error distribution of the 140-ft for wavelength  $\lambda = 1.3 \text{ cm}$  was discussed in detail by S. von Hoerner [11]. The error allocated specifically for the deformable subreflector is 0.42mm rms.

During the design of the subreflector, sources of error taken into account are:

- 1) the residual path length error after the astigmatic correction;
- 2) the deflection of the back-up frame and linkage causing an actuation differ and from the commanded magnitude;
- 3) the manufacturing inaccuracy of the subreflector surface and
- 4) the inaccuracy of the electronic control.

The first item was derived by analytical means. The difference of an astigmatic correction and the surface error of the main reflector is computed at various telescope positions. The average of these differences is found to be 0.26mm rms [1][11].

The second item was found by direct measurements after the subreflector was assembled. These measurements were obtained by placing dial indicators at various points of the frame, and recorded the deflection when the subreflector is deformed in a given amount. Due to the insufficient design of these parts, the average efficiency of the deforming system is only 60%. The averaged peak deflection of the linkage is 1.02mm, and the standard deviation is considered to be 0.34mm rms.

The surface error measured at the plant and in Green Bank produced an average value of 0.25mm rms. Refer to section "surface evaluation and measurement" for details.

The error derived from the electronics is small: 0.04mm rms. The error contributed mainly by the non-linearity of the position transducer, the temperature effect and the noise of the system. It was discussed in detail in a separate internal report by R. Lacasse [5].

All errors mentioned above are summarized in Table IV for quick reference. The combined error, a root sum square of the above mentioned contribution, is:

$$\text{Total error from the subreflector} = 0.50\text{mm} \quad (3)$$

#### Deforming the Subreflector Surface

The first order astigmatic deformation is defined by the rim deflection 'a' at four points  $90^\circ$  apart. The deflection of the circumference forms a two-cycle sine wave.

Figure 4 summarized the analytical and measured rim deflections in terms of the elevation positioning the telescope. The computations were based on the surface-panel adjustment at zero hour angle,  $+4.4^\circ$  declination, with the dish illuminated with 9 and 15 db taper. There is good agreement between the analytical curves and the measurement with narrow feed horn, in which the edge taper of 8.7 db was used. The Cassegrain feed presently used has a 10 db taper. The rim deflection of the subreflector approximates the measured curve, with 'a' defined as the rim deflection, and  $\phi$  the elevation angle of the telescope:

$$a(\text{mm}) = -1.72 + 8.70 (1-\sin \phi) \quad (4)$$

The first term gives the absolute value of rim deflection at zenith position, and the constant of the second term denotes the total rim deflection required as the telescope moves from zenith position to horizontal position. The sign convention of the rim deflection is given in Table V.

Positive denotes a deflection towards the main reflector; whereas negative denotes a deflection away from the main reflector. Plus sign means a reduction of path length, and negative an addition to the path length.

#### The Motion of the Ideal Actuators

Actuators A1 thru A4 are arranged in a circle with a radius equal to 0.99m (39 in.) from the parabolic axis. The value 'a' from the analyses, also given in Figure 4, are based on a circular aperture, in which the radius of the rim equals 1.58m (62.28 in.). The amount of actuation required for each actuator are reduced by a geometric constant  $g$  where

$$g = 39/62.28 = 0.626 \quad (5)$$

so that the amount of actuation 'd' in mm at A1 thru A4 are

$$d = a \times g = -1.078 + 5.446 (1-\sin \phi) \quad (6)$$

Since the most useful range of the telescope are positions above 20° elevation, the total amount of rim deflection  $A_o$ , taken from Figure 4, is

$$A_o = 6.8\text{mm} \quad (7)$$

The corresponding total amount of actuation  $D_o$  required at A1 thru A4 is

$$D_o = g \times A_o = 4.3\text{mm} \quad (8)$$

Evaluation and Measurements of the Subreflector Surface

The surface manufacturing tolerance specified was 0.17mm rms. The measurement at the factory during the acceptance tests was 0.24mm rms [12]. In spite of this discrepancy, the subreflector was accepted and we proceeded with the distortion tests, which was, as agreed beforehand, no longer the responsibility of the manufacturer. These additional tests indicated no noticeable hysteresis. Surface contours repeated well after three cycles of deformation.

The surface was measured again in Green Bank with the in-home designed jig. The measuring accuracy is considered higher than that of the factory, and the data was processed with a best-fit program, included in Appendix E.

The results of the nine measurements was summarized in Table VI, with detail computations in ref. [13]. The first three measurements consistantly yielded a value of 0.21mm rms. The surface became slightly degraded after some cyclic distortions. The nominal rms deviation from the best fit hyperboloid  $\Delta Z$  is considered

$$\text{rms } (\Delta Z) = 0.25\text{mm} \quad (9)$$

It is advisable to re-adjust the subreflector at times so that the value 0.25mm rms or less can be maintained. Figure 5 shows the surface contours of three measurements.

There are six dials on the template which give six readings on each radius. The readings were taken on every  $15^\circ$ , providing 24 sets of radial readings. Each surface measurements hence produced 144 single dial readings. These readings were recorded manually, and data are punched on cards as input to the computer.

The zero-readings on the template profile were done prior to each measurement. These six additional data are required by the program.

The first subreflector of the 140-ft was also measured. The purpose of this measurement was to provide the proper position of the bearings on the beam-tilting shaft, so that the alignments of these two subreflectors are "identical" when installed on the telescope. It is interesting to note that the profile of this first subreflector had deteriorated from the original error of 0.25mm rms to 0.43mm rms after four years of service [14].

#### Evaluation and Measurement of the Experimental Actuators

Equation (6) represents the amount of actuation required for each actuator at a given telescope elevation  $\phi$ . It is assumed that the actuators are supported by a perfectly rigid frame. In reality, the bending of the frame and the linkage cause a reduction of the efficiency. In order to match the input and the output, calibration constants are incorporated to each individual actuator.

The most direct way to measure the efficiency is to place a dial indicator at the surface underneath each actuator, and to compare the commanded (input through the controller) and the dial reading. The ratio of the output and the input of the four actuators are listed in the third column of Table VII.

The deflection of the frame was measured in the similar fashion. The ratio of output and input are listed in column no. 1 of Table VII.

The amount unaccounted for is considered the deflection of the linkage. These values are listed in column no. 2 of Table VII, so that the sum of the column 1 thru 3 is 100% for each actuator.

Figure 6 illustrates a comparison of commanded actuation and the measured deformation under the dial no. 4 and 6. The solid line is the measurements, whereas the dashed lines are the ideal readings, based on the locations of the dial, assuming the supporting frame and linkage are perfectly rigid. The ratio of the two different slopes at dial no. 4 indicates a reduction of efficiency. The results, called indirect measurements, are listed in the forth column of Table VII.

Figure 6 also illustrates the linearity of the subreflector surface when deformed, showing the structure is behaving in its elastic range.

The average values of the direct and indirect measurements are listed in column 5, with the invert listed in column 6.

It is clear that the linkage arms and hinges are not adequately designed. Improvement is possible and desirable..

#### The Motion of the Experimental Actuators

The actuators used for the experiment have a maximum travel  $D_0$  of 6.35mm. The range was reduced by half in order to increase the rated force from 445 N (100 lbs) to 890 N (200 lbs). Hence in theory the actuation at the output is  $D_2$ , where

$$D_2 = 6.35 \div 2 = 3.18\text{mm} \quad (10)$$

The amount given in (10) was not totally realized. The actual travel capabled through the controller is limited to a value  $D_3$  where

$$D_3 = 2.06\text{mm} + 0.50\text{mm} = 2.56\text{mm} \quad (11)$$

The zero crossing of  $D_3$  was set to 0.50mm in the controller as well as at the actuators.

The efficiencies of these actuators were measured as tabulated in Table VII. The averaged efficiency is found to be 60%. Hence the maximum travel  $D_4$ , capable by the present actuators at the output is

$$D_4 = (2.06+0.50) \times 60\% = 1.24+0.30=1.54\text{mm} \quad (12)$$

The corresponding rim deflection  $A_3$ , due to the ranges of the actuators described in (12) is

$$\begin{aligned} A_3 &= (1.24 + 0.30)/0.626 \\ &= 1.98 + 0.48 \\ &= 2.45\text{mm} \end{aligned} \quad (13)$$

The amount of (13) is marked in Figure 4. Compared with demanded range of 6.8mm eq. (7), the present actuators are short of the design goal by a factor of 2.8.

### III. DEFORMING SYSTEM

#### General Description

The deformation of the subreflector is controlled by four independent and identical systems. Each system controls the contour of one quadrant of the surface. Each system has its own position control. The influence of deformation in one quadrant to the others is reduced because of the two stiff diagonals on the back of the subreflector (Figure 1).

The deforming system has four major parts: an electronic control, a position transducer, a motor actuator and a lever arm linkage. The first three items are covered in the internal report 139 in detail by R. Lacasse [5]. The lever arm linkage is illustrated in a detail drawing, no. 30D00017 in Appendix C.

This deforming system is an experimental version. Once this deformable subreflector is proven workable, the deforming system should be modified to incorporate actuators with a larger amount of actuations. A reverse in the direction of actuation will make the subreflector more versatile: it will be usable for receivers placed  $\pm 90^\circ$  and  $180^\circ$  apart from the present K-band maser receiver location.

#### Electronic Control

For the completeness of this report, a block diagram of the control system is included for reference, illustrated in Figure 7. Each actuator's position is monitored by a LVDT (Linear Voltage Displacement Transducer). A position given by the computer is compared with the measured position.

The difference of these quantities is reduced to an amount of  $\pm 0.01m$ . The commanded position is up-dated by the output of the computer while the telescope tracks a source. The up-date rate is set to be 1 new position per second.

Figure 8 shows the front panel of the controller. The controller is an interface between the H-316 on-line computer and the servo mechanism. It's functions are receiver and transmitter data. Presently this interface is connected to the power supply at the focus by cable and no. 45 and 34 in the control room.

The interface provides the option of manual and computer control. A switch for this selection is located in the upper center of the panel.

Upper travel limit of 2.56mm is displayed under this switch. A display of travel in mm is located below this 'limit' window, with the selecting switch located on the right.

It is possible to monitor the commanded and measured positions of actuators A1 thru A4. It is also possible to monitor the temperature at the LVDT in Celsius. Heating elements are provided to the position transducer to maintain continued level specified by the producer of the transducer.

The display of 'LOCK' is for debug purposes. It shows the differences between the sum of the commanded positions and the sum of the actual positions.

The manual control enables one to input values into the thumb wheel knobs, either individually or as a group (switch to 'ALL'). The step is executed by pressing the 'UPDATE ENABLE' button.

All actuators are travel from an undeformed position to a predetermined direction (see Table V). The deforming option is applicable only for the K-band maser receiver.

#### Force Requirement on Actuation

The size of the actuator depends on 1) the force required to produce the given amount of deformation on the subreflector; 2) the weight of the subreflector surface and 3) the dynamical force due to the periodic tilt of the subreflector in the beam-tilting mode.

As shown in eq. (8), the range of actuation from 20° elevation angle to 90°, based on the measured value of astigmatism, is 4.3mm. Refer to eq. (2), that the stiffness of the shell structure when actuated in a astigmatic deflection, is 201 N/mm. The force required for the full actuation is

$$F \text{ (astigmatic)} = 4.3\text{mm} \times 201 \text{ N/mm} = 864 \text{ N}(194 \text{ lb}) \quad (14)$$

The weight of the shell is 668 N (150 lbs). Assuming that the weight is equally distributed to the eight connections, the force on the actuator due to dead weight is

$$F \text{ (dead weight)} = 668 \text{ N}/8 = 83 \text{ N} (19 \text{ lb}) \quad (15)$$

The force due to the beam switching at  $\lambda = 2.0 \text{ cm}$  is derived as follows:

$$B \text{ (HPBW)} = 1.2 \lambda/D = 57.92 \lambda \text{ (sec)}$$

$$\theta \text{ (beam tilt)} = 3B$$

$$\alpha \text{ (Rotation of the subreflector)} = \frac{\theta \times M}{1.15} = 8.13 \theta$$

$$\tau \text{ (transition time)} = 40 \text{ ms}$$

$$T \text{ (available torque)} = 7000 \text{ ft-lb}$$

$$A \text{ (angular acceleration)} = \frac{4\alpha}{\tau^2} = 34.3 \text{ rad/sec}^2$$

$$m \text{ (mass of the shell per connection)} = 150\text{lb}/8 = 19 \text{ lb} = .049 \frac{\text{lb} - \text{sec}^2}{\text{in}}$$

$$d \text{ (distance to the axis of tilt)} = 39 \text{ in}$$

$$F \text{ (beam tilt)} = m \cdot A \cdot d = 294\text{N} \text{ (66 lb)} \quad (16)$$

The total force required for each actuator is the sum of the force shown in eq. (14), (15) and (16), or

$$F \text{ (total)} = 864+83+294 = 1241\text{N}(279 \text{ lb}) \quad (17)$$

The experimental version has actuators rated at 100 lbs. This force was amplified by a factor of 2 by lever arm linkage, having rated output of only 200 lbs.

#### Type of the Experimental Actuator

The size of the actuator is dependent on the required force as described in eq. (17) and the amount of actuation as in eq. (8). The available actuator for the experimental version of the deformable subreflector has the following properties:

Manufacturer:	AIRSEARCH
Part No.:	34596
Weight (approx.):	2.5 lbs.
Max. Actuation:	0.25 in (6.35 mm)
Max. Load:	100 lb (445 N)
Motor Type:	Series wound
Electrical:	20 VDC

The Linkage

The necessity of this linkage is due to the motor actuator available, in conjunction with the requirement in force and displacement of the sub-reflector. The final version of the deforming system could by-pass this linkage to reduce the additional deflections.

The extension of the lever arm also provides an amplification in the travel of the LVDT.

The Switching Off of the Actuators

The subreflector deformation can be terminated either at the commencement of an observation; or if erratic behavior is detected, such as the monitored amount of actuation being different from the commanded quantities; or the temperature readings at the actuator motors show a level higher than a preset value.

The proper sequence is 1) to set all actuator command values to 0.50 mm at the four windows on the left hand side of the panel; 2) switch the "manual/computer" switch to the manual position; 3) put the update selection button to "all" position and 4) press the "update enable" button. This will activate all actuators to drive the surface back to the undeformed position. These positions will hold even if the power supply is turned off.

## IV. BACKUP FRAME

General Description

The backup frame of the deformable subreflector provides the following functions: to add structural stiffness to the subreflector; to interface the subreflector to the existing beam tilting device; and to support the actuators-linkage combinations.

The subreflector is connected to the frame at eight points. Four of which are actuated by electro-mechanical devices, labeled as A1 thru A4. Another four connections are mechanically fixed with rods and brackets, and labeled as S1 through S4. Figure 1 shows the schematic arrangements of these connections, and appendix B shows the detail. The stationary and the actuated connections are alternately arranged for the astigmatic deformation of the subreflector.

The subreflector-frame combination is attached to the beam tilting device through two bearings and two connections to the push rods. These connections are designed for quick installation so that the telescope can be operated in either prime focus or Cassegrain system. All connections are positioned beforehand by pins so that calibration procedures are kept to a minimum after the subreflector is installed.

The Design

The material of the frame is aluminum. The limit of design is not governed by the allowable stress but by the total weight and moment of inertia. The detail of the design is included in Appendix B. The analyses of the structure is summarized from the detailed computation of reference [8] and listed as follows:

## Properties of the Subreflector Frame

Weight	6 in. sch. 10 weldment Brackets Shaft & brgs	134.4 lb 63.0 lb 83.0 lb
	Total	286.4 lb
Moment of Inertia	About the Shaft	$3 \times 10^4$ lb-in <sup>2</sup>
Spring const. in the direction parallel to the telescope axis	A1, S2, A3, S4: 2.05x10 <sup>4</sup> #/in S1, A2, S3, A4: 6.29x10 <sup>4</sup> #/in	
Max. bending stress		612 psi
Max. shear stress		84 psi
Resonance frequency	Frame alone With Subreflector	105 Hz 33 Hz

The frame was fabricated in the G.B. shop. It was shipped to ASI of California for the framing of the subreflector. The subreflector/frame combination was shipped back to G.B. as one integral part.

## V. SOFTWARE PROGRAMMING

### General Description

A subroutine was added to the 140-ft telescope control program in the Honeywell-316 computer by Bob Vance. This subroutine gives the user the option of using this deformable subreflector by switching on the power supply of the servo control electronics and setting the manual/computer switch (see fig. 8) to the computer control mode.

This subroutine was written based on the algorithm illustrated in figure 9.

### The Input and The Output

The amount of actuations on the subreflector surface is dependent on the elevation angle  $\phi$  of the telescope. The values  $\phi$  are readily calculated by the main control program.

There are four outputs from this subroutine: a, b, c and d. Each is a eight-bit word, containing a max. value of 255. These outputs are channeled to the controller, and ultimately translated into displacements of the subreflector shell. The expressions in eq. (18) are modifications of eq. (6), with zero crossing set at 0.50 mm:

$$\begin{aligned}
 P_1 &= V_1 + V_2 (1-\sin \phi) = -0.578+5.446 (1-\sin \phi) \\
 P_2 &= V_3 + V_4 (1-\sin \phi) = 0. \\
 P_3 &= V_5 + V_6 (1-\sin \phi) = 0. \\
 P_4 &= V_7 + V_8 (1-\sin \phi) = 0.
 \end{aligned} \tag{18}$$

and subsequently, the four output words are expressed as:

$$\begin{aligned}
 a &= (P_1 + P_2 + P_3) \times C_1 \text{ at } A_1 \\
 b &= (P_1 + P_2 - P_3) \times C_3 \text{ at } A_3 \\
 c &= (-P_1 + P_2 + P_4) \times C_2 \text{ at } A_2 \\
 d &= (-P_1 + P_2 - P_4) \times C_4 \text{ at } A_4
 \end{aligned} \tag{19}$$

$P_1$  represents the first order astigmatic deformation.  $P_2$  thru  $P_4$  are values for higher order deformations, which are not being considered during the design phase of the subreflector. Presently  $P_2$  thru  $P_4$  are dummies and the values of  $P_2$  thru  $P_4$  (or  $V_3$  thru  $V_8$  in eq. (18)) are set to zero. These values can be redefined once it is proven that the subreflector is capable of these types of deformations.

$C_1$  thru  $C_4$  are calibration constants, correspondent to actuators  $A_1$  thru  $A_4$ . The numerical values of  $C_1$  thru  $C_4$  are listed in table VII, column 6.

## VI. MEASURING JIG

Fig. 10 shows the general setup of the measuring jig, with the detailed design included in Appendix D. It consists of a supporting frame for the subreflector and a template. The measuring jig serves the following purposes.

- 1) to verify the subreflector's surface accuracy,
- 2) to measure the contour of the deformed subreflector,
- 3) to evaluate the efficiency of the actuators, and
- 4) to provide a reference system for future adjustments.

The subreflector was held in place and was so adjusted that its hyperbolic axis is aligned with gravity. The central axis of the jig is defined by an optical plumb, with the three adjustment screws at the supporting legs to correct the tilt, and mild forces required to shift the jig in lateral direction so that the axes of the subreflector and the jig are coinciding. Few repeating cycles are required until these two axes will actually meet. The optical plumb defines the direction of gravity, and with an eyepiece to collimate the central mirror of the subreflector.

The horizontal reference of the template was monitored by an optical level (Wild N3) to insure the line remains horizontal as the jig rotates. There is no fine adjustment for the counter weight, but good balance can be achieved by using heavy bolts or nuts clamped on the jig.

The 1/8 inch steel plate template has a cut-out hyperbolic profile. This profile was also measured by optical means so that the reference is well established. Fig. 11 shows the arrangements of the dial indicators, the reference profile and the proper corrections for the zero readings of each dial.

The dials are placed on the template vertically. The dials are product of MITUTOYO, part no. 3052. The graduation is 0.010 mm. The total travel is 30 mm.

There was no effort to evaluate the accuracy of the system. Rough estimates of the measure accuracy is about ± 0.050 mm.

#### ACKNOWLEDGEMENT

The author wishes to thank the Green Bank workshop, under the supervision of Albert Steinemann and Martin Barkley, for the assembly of the subreflector stiffening frame; the maintenance group with Ron Gordon, Don Gordon and Herb Hanes for the mechanical work; Sidney Smith for the help during the measurement of the surface. The Controller was designed and assembled by R. Lacasse of the Electronic Division. R. Vance was responsible for the programming. Also thanks for advice from R. Fisher. The moving force of the project shall be accredited entirely to Dr. S. von Hoerner.

## REFERENCE

- [1] S. von Hoerner and W-Y. Wong, "Gravitational Deformation and Astigmatism of Tilttable Radio Telescopes", IEEE Trans. Antennas Propagat., Vol. AP-23, pp. 689-695, 1975.
- [2] S. von Hoerner, "The Design of Correcting Secondary Reflectors," IEEE Trans. Antennas Propagat., Vol. AP-24, pp. 336-340, 1976.
- [3] P. R. Cowles and E. A. Parker, "Reflector Surface Error Compensation in Cassegrain Antennas," IEEE Trans. Antennas Propagat., Vol. AR-23, p. 323, 1975.
- [4] S. von Hoerner, "Measuring the Gravitational Astigmatism of a Radio Telescope," IEEE Trans. Antennas Propagat., Vol. AP-26, pp. 315-318, 1978.
- [5] R. J. Lacasse, "Correctable Subreflector Controller," N.R.A.O. Electronic Division Internal Report No. 193, 1978.
- [6] S. von Hoerner, R. Fisher, W-Y. Wong, "140-ft Observations with Deformable Subreflector," N.R.A.O. Engineering Division Internal Report No. 109, 1978.
- [7] Peter J. Napier, "Cassegrain System for 140-ft Telescope," N.R.A.O. Memo, 1972.
- [8] Computer output file no. DS-001, "N.R.A.O. Stren Analyses of the Subreflector".
- [9] Computer output file no. DS-002, "C.D.C. Stress Analyses of the Subreflector, Dec. 28, 1976.
- [10] C.D.C. Report, "Stress Analyses of A Deformable Subreflector", Control Data Corp., Dec. 28, 1976.

- [11] S. von Hoerner, "140-ft Deformable Subreflector", N.R.A.O. Memo, October 28, 1975.
- [12] Computer output file no. DS-004, "Antenna System Inc. Surface Measurement",
- [13] Computer output file no. DS-005, "Green Bank Measurements of the Deformable Subreflector".
- [14] Computer output file no. DS-003, "Green Bank Measurements of the First Subreflector".

## LIST OF TABLES

- TABLE I SUBREFLECTOR EDGE COORDINATES. DEFINITION OF ANGLE  $\phi$  IS SHOWN IN FIG. 7, LINEAR DIMENSIONS ARE IN INCH
- TABLE II MATERIAL LIST OF THE SUBREFLECTOR
- TABLE III ANALYTICAL RESULTS BY CDC
- TABLE IV ERROR CONTRIBUTION OF THE SUBREFLECTOR
- TABLE V LOCATION AND SIGN CONVENTION OF THE ACTUATIONS
- TABLE VI G. B. MEASUREMENTS OF THE SUBREFLECTOR SURFACE
- TABLE VII EFFICIENCY OF THE ACTUATORS

TABLE I. SUBREFLECTOR EDGE COORDINATES. DEFINITION OF ANGLE  $\phi$  IS SHOWN IN FIG. 1, LINEAR DIMENSIONS ARE IN INCH

$\phi$	R	Z(R)	$\phi$	R	Z(R)
-90.000	67.842	19.187	0.0	61.996	16.133
-88.000	67.839	19.185	2.000	61.803	16.036
-86.000	67.827	19.179	4.000	61.610	15.940
-84.000	67.809	19.169	6.000	61.419	15.844
-82.000	67.783	19.155	8.000	61.229	15.749
-80.000	67.749	19.137	10.000	61.040	15.656
-78.000	67.708	19.114	12.000	60.853	15.563
-76.000	67.660	19.088	14.000	60.669	15.472
-74.000	67.605	19.058	16.000	60.486	15.383
-72.000	67.543	19.025	18.000	60.306	15.294
-70.000	67.473	18.987	20.000	60.129	15.207
-68.000	67.397	18.946	22.000	59.954	15.122
-66.000	67.314	18.901	24.000	59.783	15.038
-64.000	67.224	18.853	26.000	59.614	14.956
-62.000	67.128	18.801	28.000	59.449	14.877
-60.000	67.025	18.746	30.000	59.288	14.799
-58.000	66.916	18.688	32.000	59.130	14.722
-56.000	66.801	18.626	34.000	58.976	14.648
-54.000	66.681	18.561	36.000	58.827	14.576
-52.000	66.554	18.494	38.000	58.681	14.507
-50.000	66.422	18.424	40.000	58.540	14.439
-48.000	66.285	18.350	42.000	58.403	14.374
-46.000	66.143	18.275	44.000	58.271	14.311
-44.000	65.995	18.197	46.000	58.143	14.250
-42.000	65.843	18.116	48.000	58.020	14.192
-40.000	65.687	18.034	50.000	57.903	14.136
-38.000	65.526	17.949	52.000	57.790	14.083
-36.000	65.362	17.862	54.000	57.683	14.032
-34.000	65.194	17.774	56.000	57.580	13.984
-32.000	65.002	17.684	58.000	57.484	13.939
-30.000	64.847	17.593	60.000	57.392	13.896
-28.000	64.668	17.500	62.000	57.306	13.855
-26.000	64.487	17.406	64.000	57.226	13.817
-24.000	64.30	17.310	66.000	57.151	13.783
-22.000	64.117	17.214	68.000	57.082	13.750
-20.000	63.930	17.117	70.000	57.019	13.721
-18.000	63.741	17.020	72.000	56.962	13.694
-16.000	63.550	16.921	74.000	56.911	13.670
-14.000	63.357	16.823	76.000	56.865	13.649
-12.000	63.164	16.724	78.000	56.826	13.631
-10.000	62.970	16.825	80.000	56.792	13.615
- 8.000	62.775	16.526	82.000	56.765	13.602
- 6.000	62.580	16.428	84.000	56.744	13.593
- 4.000	62.386	16.329	86.000	56.728	13.585
- 2.000	62.191	16.231	88.000	56.719	13.581
			90.000	56.716	13.580

TABLE II. MATERIAL LIST OF THE SUBREFLECTOR

Item	Product	Part No.
Epoxy resin and curing agent	HEXCEL	Hexcelite HP-302
Fiberglass cloth	J. P. STEVENS	No. 141
Honeycomb core	HEXCEL	5052/F40-0013-2.1
Collimating mirror	BRUNSON	185-1

TABLE III. ANALYTICAL RESULTS BY CDC

Loading Condition	Reaction at actuator N(1b)
Astigmatic correction of 1.57 mm	16 (71)
Survival load of 3.8 mm	80 (356) *
Beam tilt at 34.4 rad/sec <sup>2</sup>	4 (16)
ΔT = 10°F	3 (12)

\* Safety margin is 63% for the laminates, 54% for the core.

TABLE IV. ERROR CONTRIBUTION OF THE SUBREFLECTOR

Source	Error (mm rms)
Residue path length error after astigmatic correction	0.26
Deflection of the frame, linkage	0.34
Manufacturing error of the surface	0.25
Electronic	<u>0.04</u>
TOTAL	0.50

TABLE V. LOCATION &amp; SIGN CONVENTION OF THE ACTUATORS

+: deflect towards the main reflector to shorten the path length

-: deflect away from the main reflector to lengthen the path length

Actuator	Location	Edge Movement
A1	North	-a
A2	West	+a
A3	South	-a
A4	East	+a

TABLE VI. G. B. MEASUREMENTS OF THE SUBREFLECTOR SURFACE

Date	Measurement	Error (mm rms)	Actuation (mm)
12- 5-77	GB2-2	0.21	--
12- 7-77	-3	0.21	--
12-13-77	-4	0.21	--
12-14-77	-5	--	2.54
12-14-77	-6	0.26	--
3-15-78	-12	0.22	--
3-15-78	-13	0.26	--
3-15-78	-14	--	1.94
3-15-78	-15	0.24	--

TABLE VII. EFFICIENCY OF THE ACTUATORS

Actuator	Frame Deflection 1	Linkage Deflection 2	Direct Measurement 3	Indirect Measurement 4	Avg 5	Calibration Constant 6
A-1	16%	26%	58%	63%	60%	$C_1 = 1.67$
A-2	17%	25%	58%	62%	60%	$C_2 = 1.67$
A-3	18%	15%	67%	69%	68%	$C_3 = 1.47$
A-4	15%	35%	50%	54%	52%	$C_4 = 1.92$
					Avg 60%	

#### FIGURE CAPTIONS

- Figure 1 Schematic drawings of the arrangements of the 140-ft telescope Cassegrain system. The general dimension of the deformable subreflector is given, and its relative position to the main reflector when the K-band maser receiver is in use.
- Figure 2 Finite element model used by C.D.C., contains 180 elements, 108 nodes. The subreflector is considered symmetrical, actuated at nodes no. 52 and 62, and held at no. 57.
- Figure 3 Comparison of the deformed subreflector profile to the best-fit deviation of the main reflector at elevation angle of 28° with the radius of the main reflector normalized to 62.3 inches.
- Figure 4 Comparison of rim deflection of the deformable subreflector with the telescope positions. Dashed line denote the analytical results of 0 db, 9 db and 15 db edge taper. Solid line shows the measured result with an elongated feed.  $A_0$  denotes the desirable range of rim deflection;  $A_3$  shows the range presently covered by the experimental actuators.
- Figure 5 Profile contour of measurements GB2-4, GB2-14 and GB2-15, with contour level of 0.005 inch.
- Figure 6 Comparison of the commanded actuations (vertical scale) and measured deflections (horizontal scale). Solid line is the measurement, dashed line is the ideal.

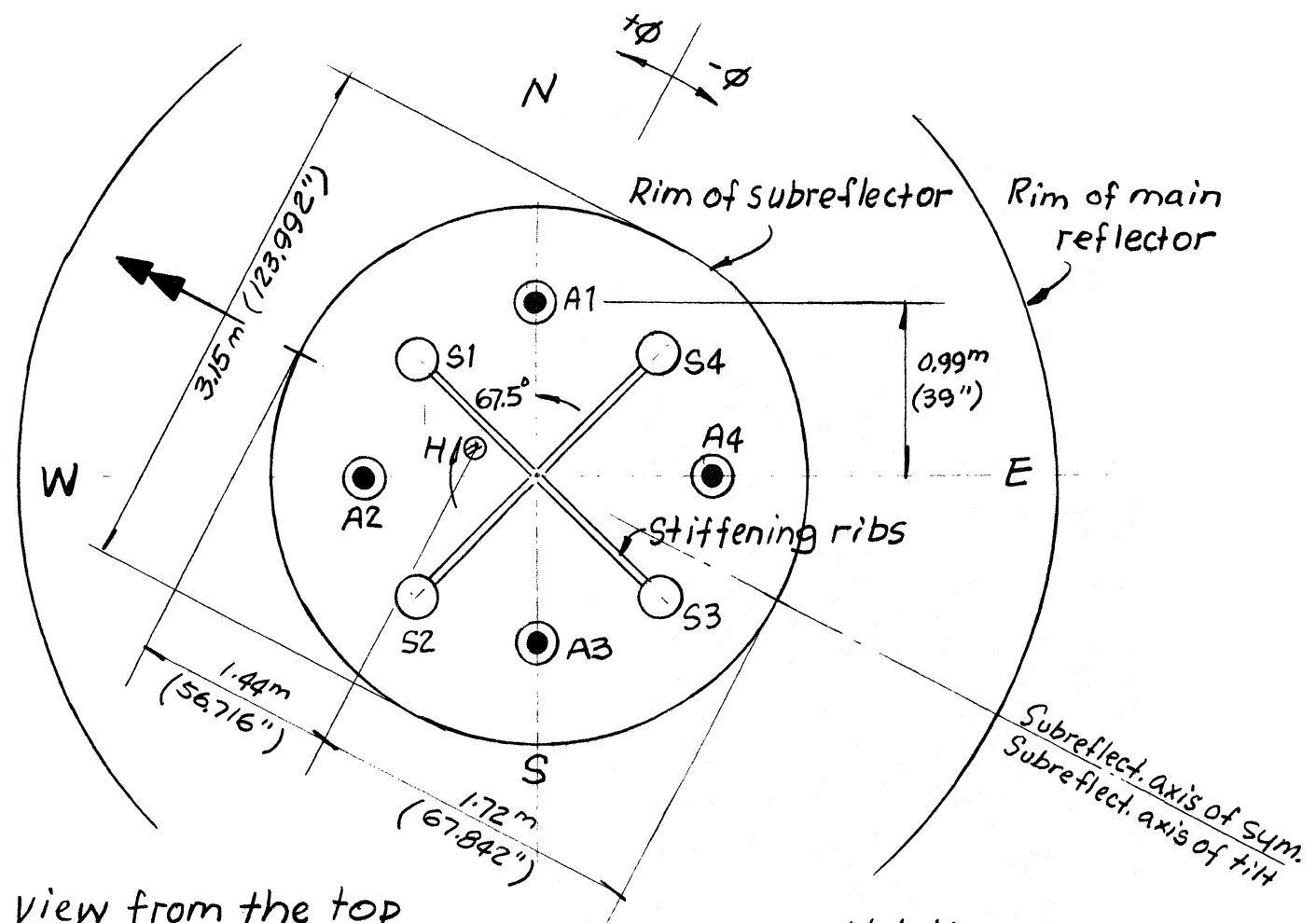
Figure 7 Deformable subreflector's electronic block diagram.

Figure 8 Panel arrangement of the controller.

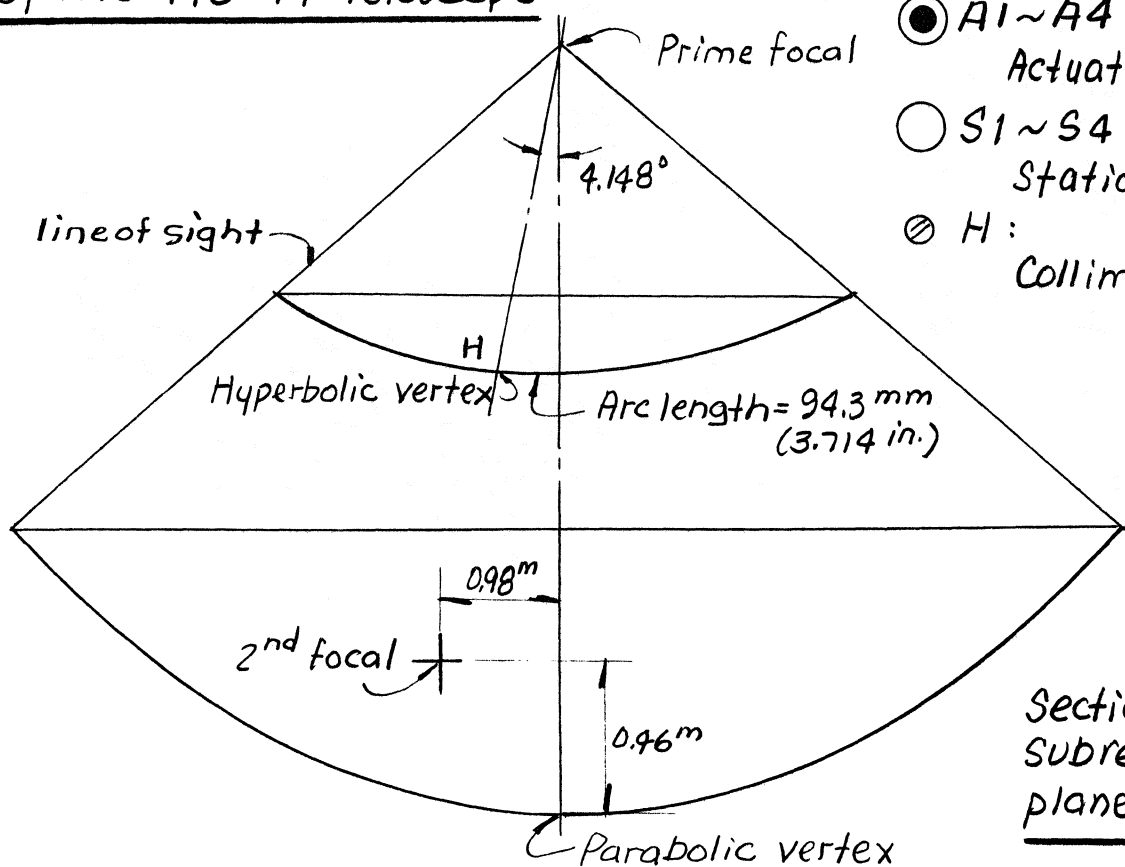
Figure 9 Subroutine flow chart implemented to the telescope control program.

Figure 10 Green Bank measuring jig for the deformable subreflector. It includes a supporting frame (1), a template (2), 6 dial indicators (3), optical plumb (4) and a rotating arm with counter wt (5).

Figure 11 The error on the profile and the reference system of the template used in the measurement.



View from the top  
of the 140'-ft telescope



#### Notation

- A<sub>1</sub>~A<sub>4</sub>: Actuated supports
- S<sub>1</sub>~S<sub>4</sub>: Stationary supports
- ◎ H: Collimating mirror

Fig. 1

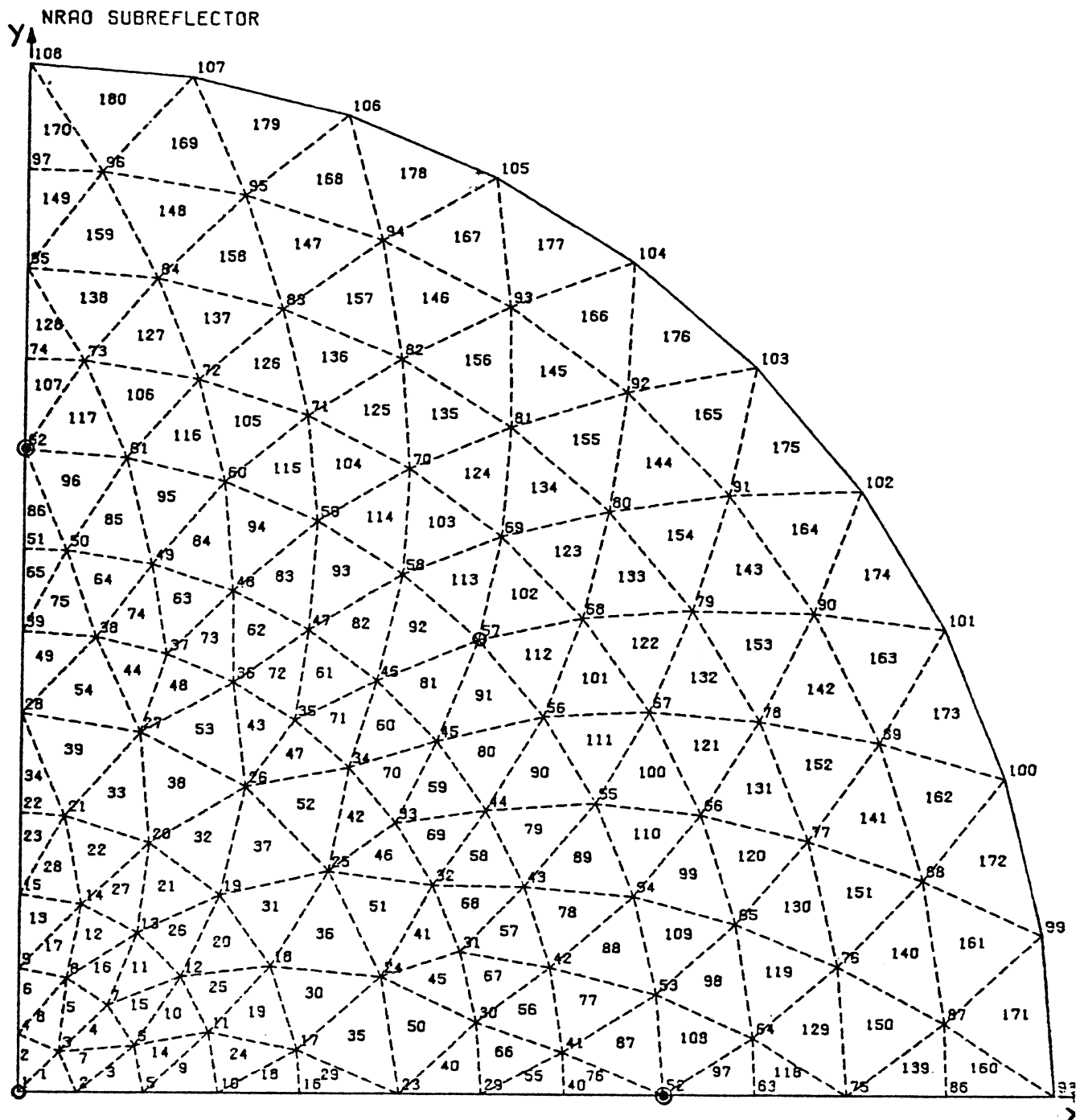


Figure 2 Finite element model used by C.D.C., contains 180 elements, 108 nodes. The subreflector is considered symmetrical, actuated at nodes no. 52 and 62, and held at no. 57.

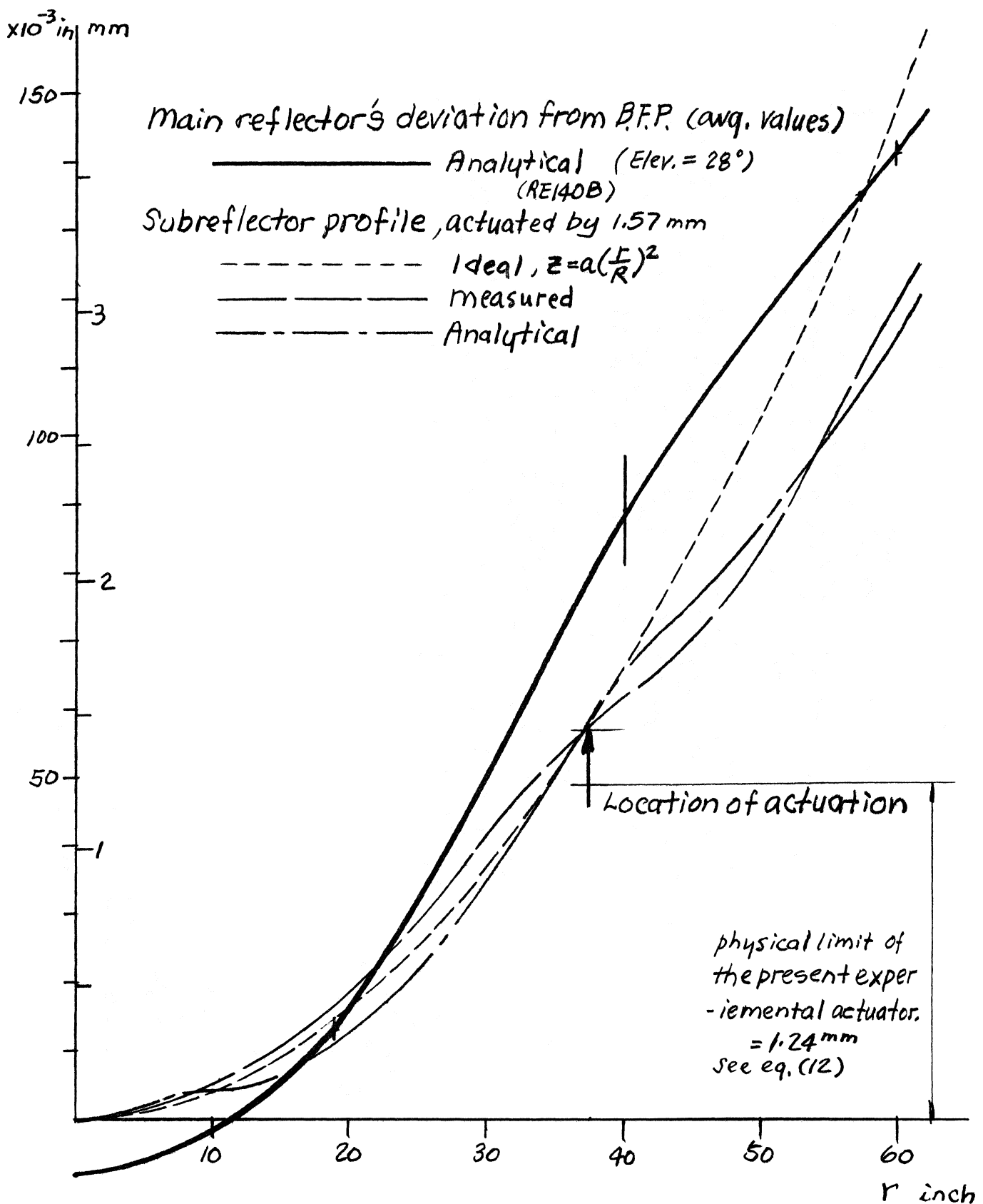


Figure 3 Comparison of the deformed subreflector profile to the best-fit deviation of the main reflector at elevation angle of  $28^\circ$  with the radius of the main reflector normalized to 62.3 inches.

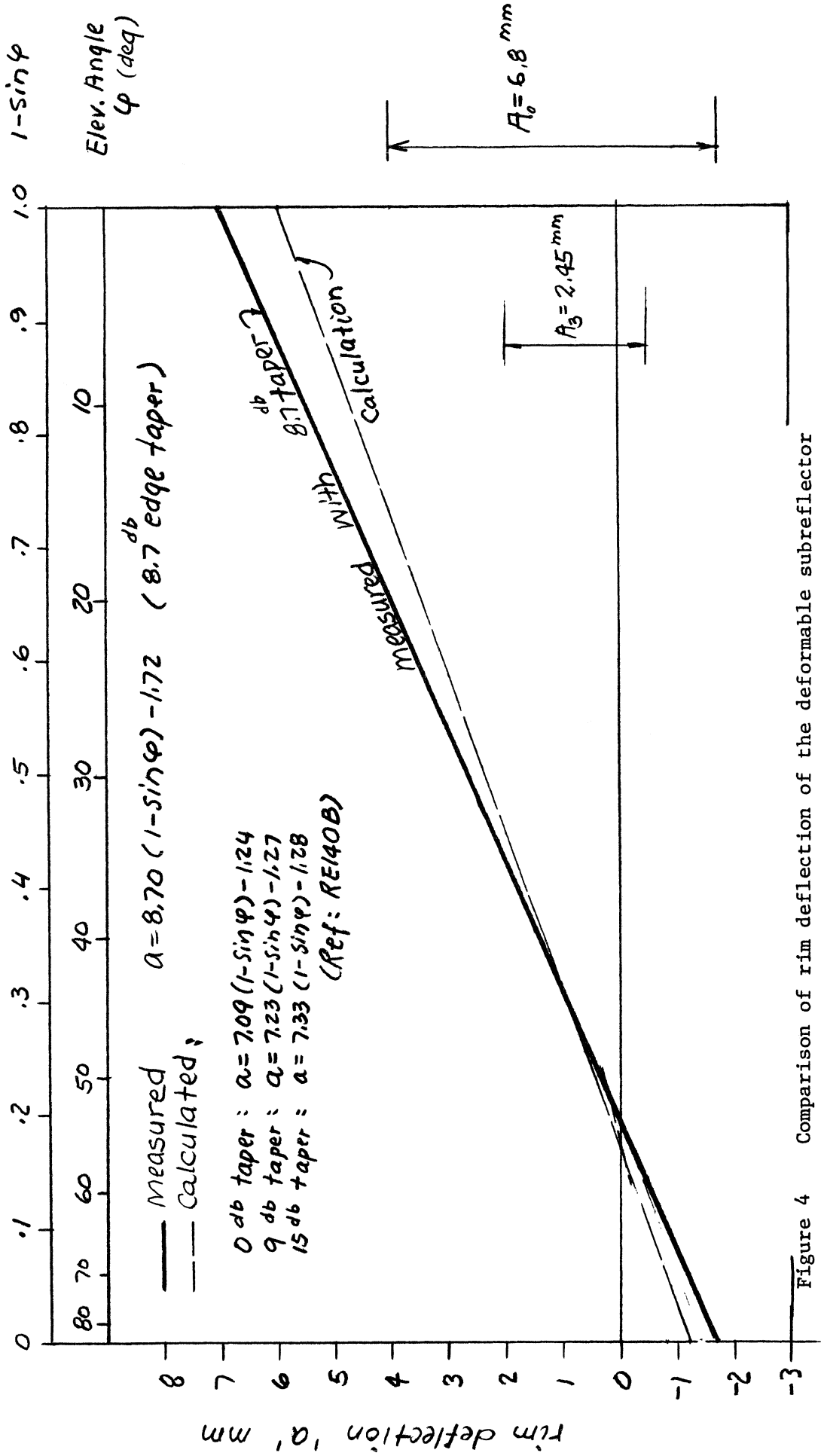
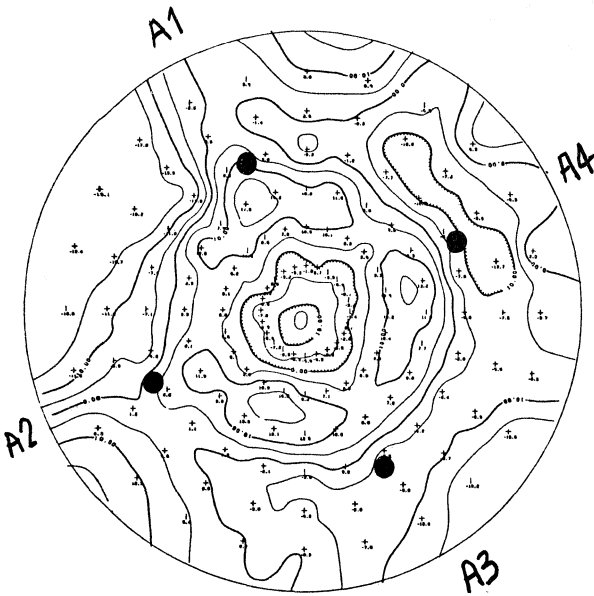


Figure 4 Comparison of rim deflection of the deformable subreflector with the telescope positions. Dashed line denote the analytical results of 0 db, 9 db and 15 db edge taper. Solid line shows the measured result with an elongated feed.  $A_0$  denotes the desirable range of rim deflection;  $A_3$  shows the range presently covered by the experimental actuators.



Measurement No.      Best-fit parameters

GB2-4

Relaxed surface

Surface error = 0.21 mm rms

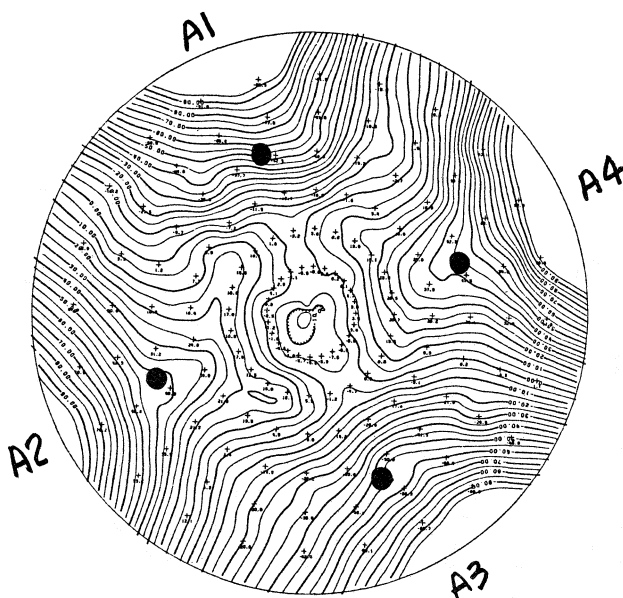
$$\Delta x = 0.04 \text{ mm}$$

$$\Delta y = 0.05 \text{ mm}$$

$$\Delta z = 7.77 \text{ mm}$$

$$\theta_x = 27.1 \times 10^{-5} \text{ rad.}$$

$$\theta_y = 2.5 \times 10^{-5} \text{ rad.}$$



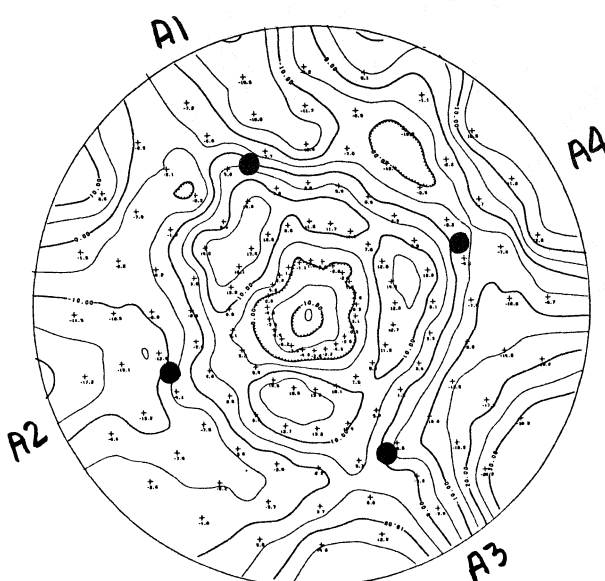
GB2-14

Deformed surface

$$A_1, A_3 = -1.94 \text{ mm}$$

$$A_2, A_4 = +1.94 \text{ mm}$$

Where '-' means lengthen of path length, and '+' shortening of Path length.



GB2-15

Relaxed surface

Surface error = 0.24 mm rms

$$\Delta x = 0.02 \text{ mm}$$

$$\Delta y = 0.04 \text{ mm}$$

$$\Delta z = 8.13 \text{ mm}$$

$$\theta_x = -40.2 \times 10^{-5} \text{ rad.}$$

$$\theta_y = 29.0 \times 10^{-5} \text{ rad.}$$

Fig. 5

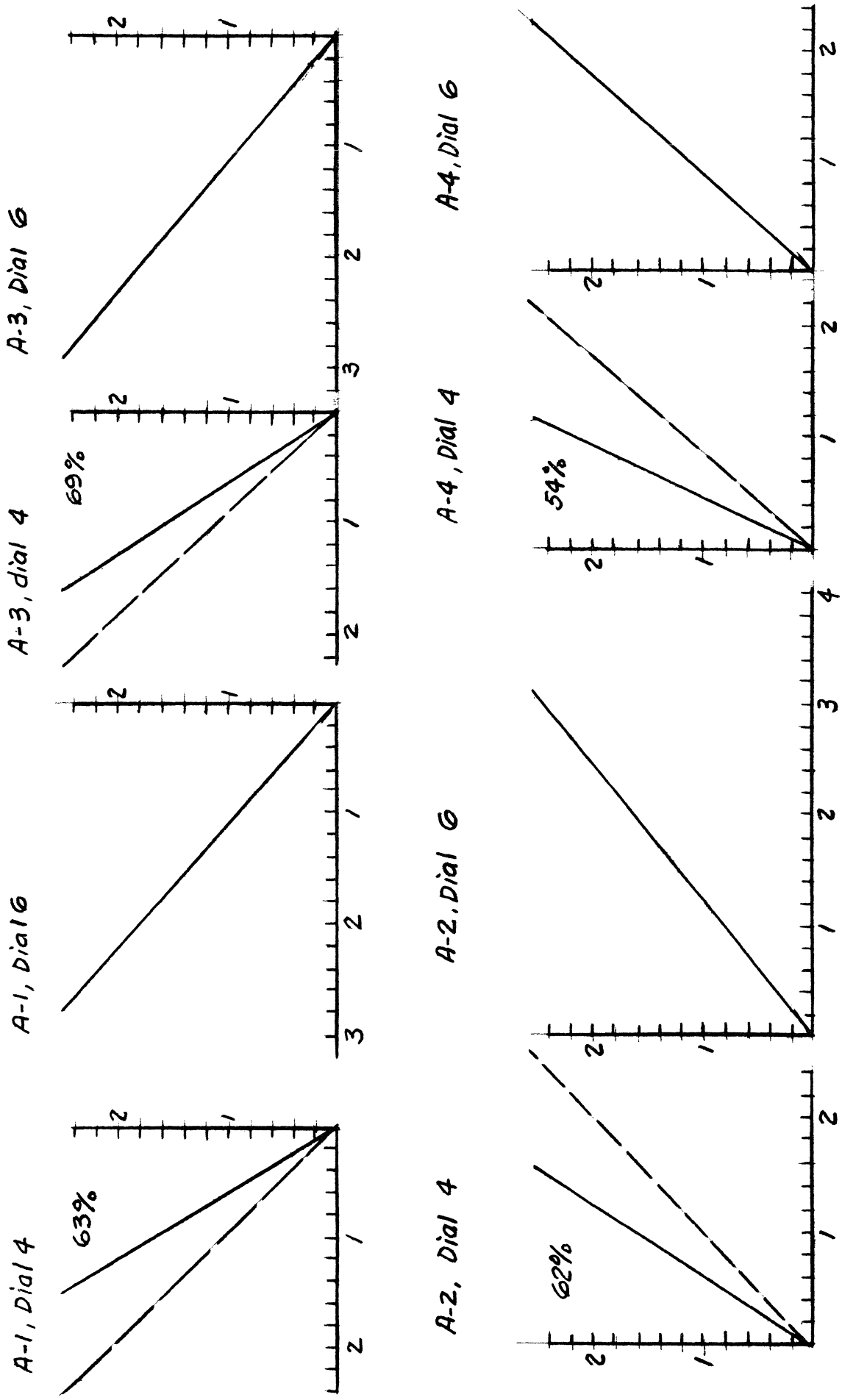


Fig. 6 Comparison of commanded actuations (vertical scale) & measured deflections (horizontal scale). Solid line is the measurement, dash line is the ideal.

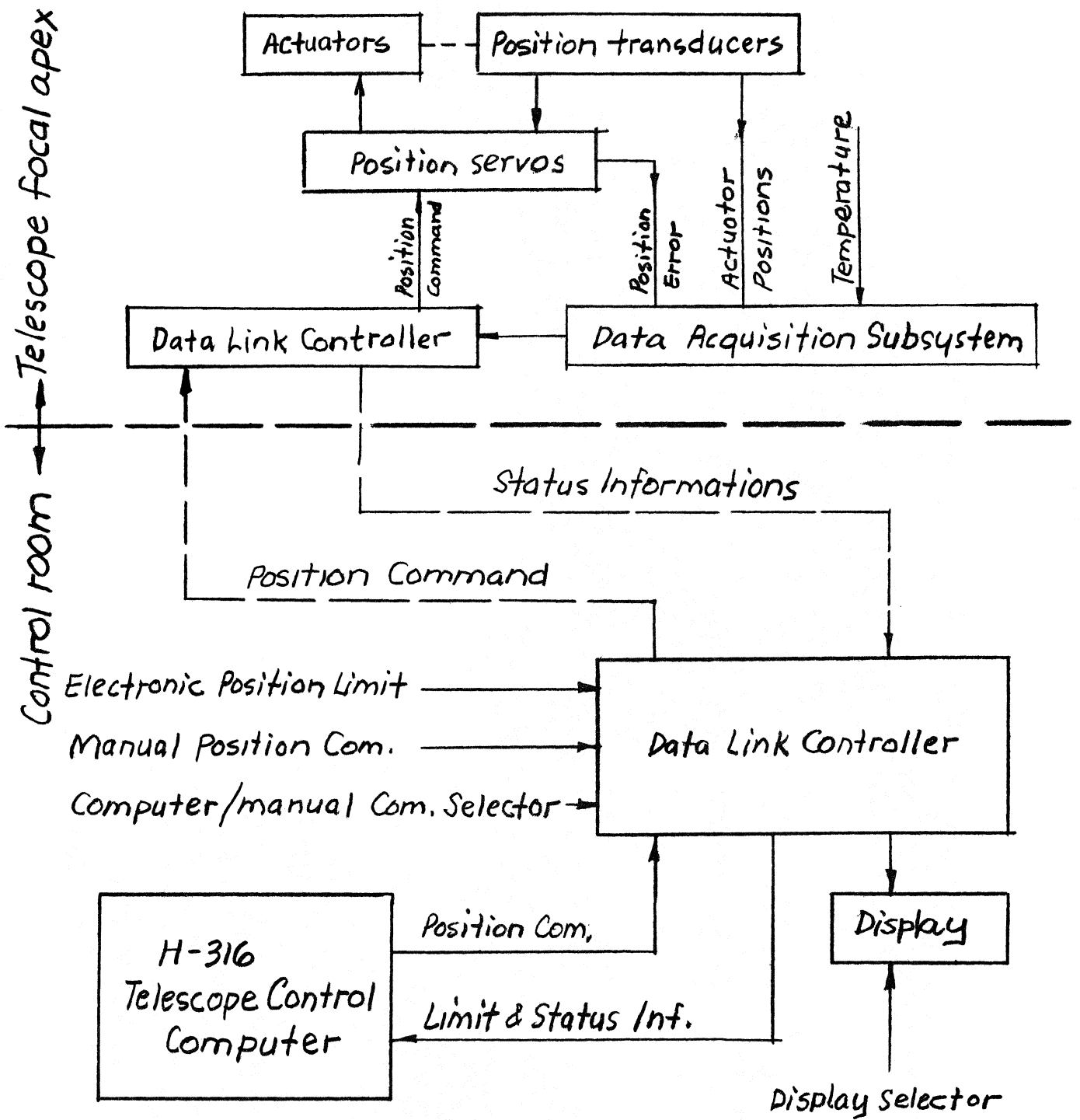


Fig. 7 Deformable Subreflector's electronic Block Diagram

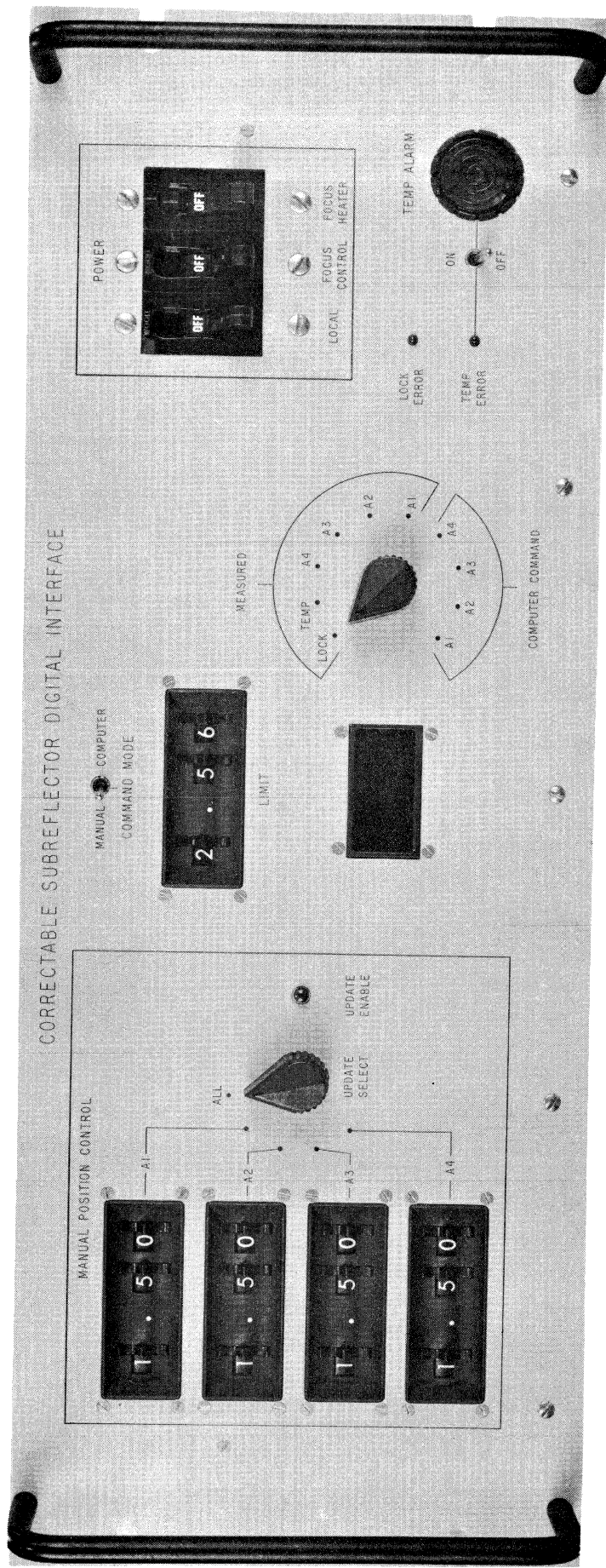


Figure 8 Panel arrangement of the controller.

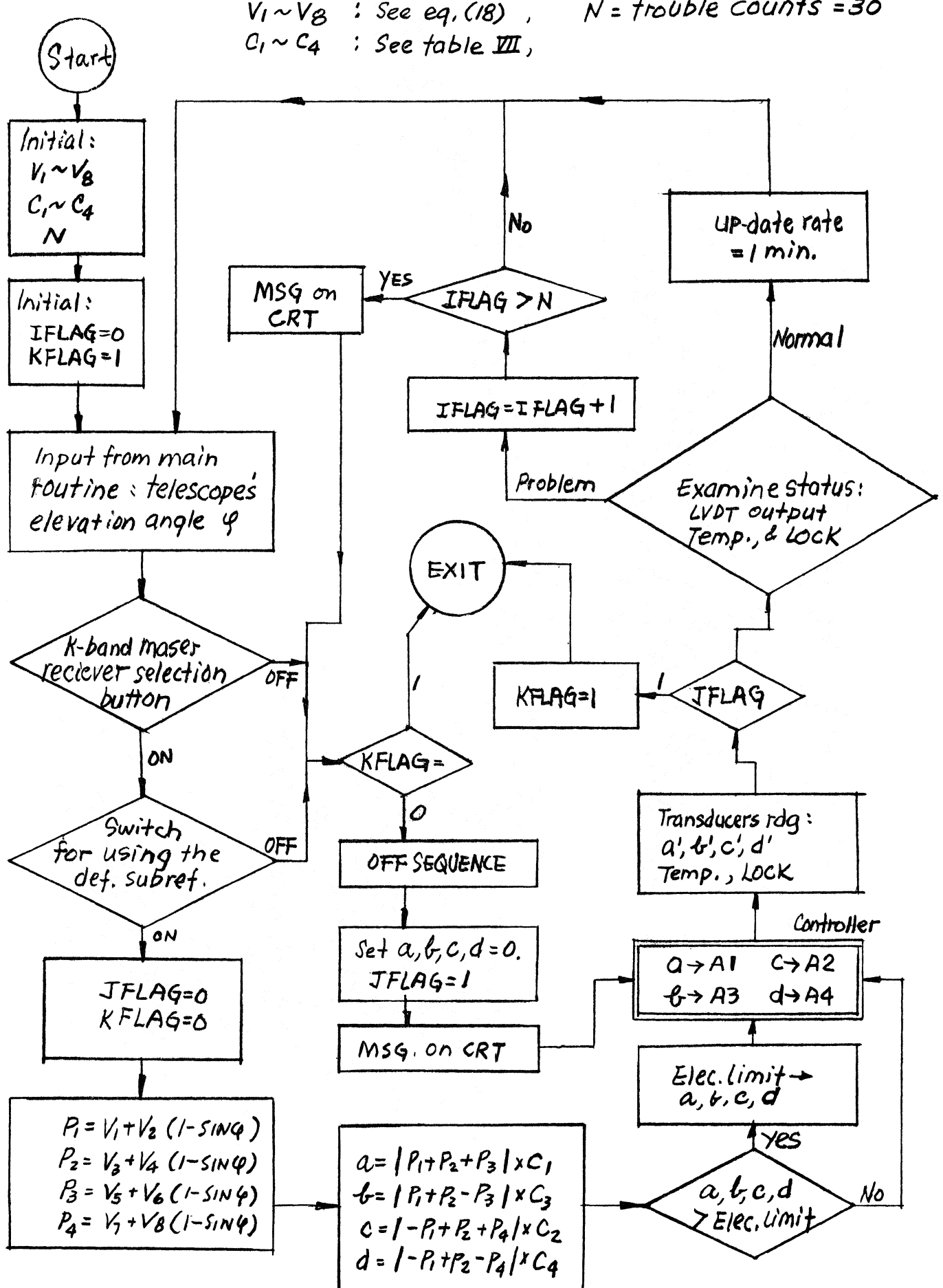


Fig. 9

Figure 10 Green Bank measuring jig for the deformable subreflector.

It includes a supporting frame (1), a template (2), 6 dial indicators (3), optical plumb (4) and a rotating arm with counter wt (5).

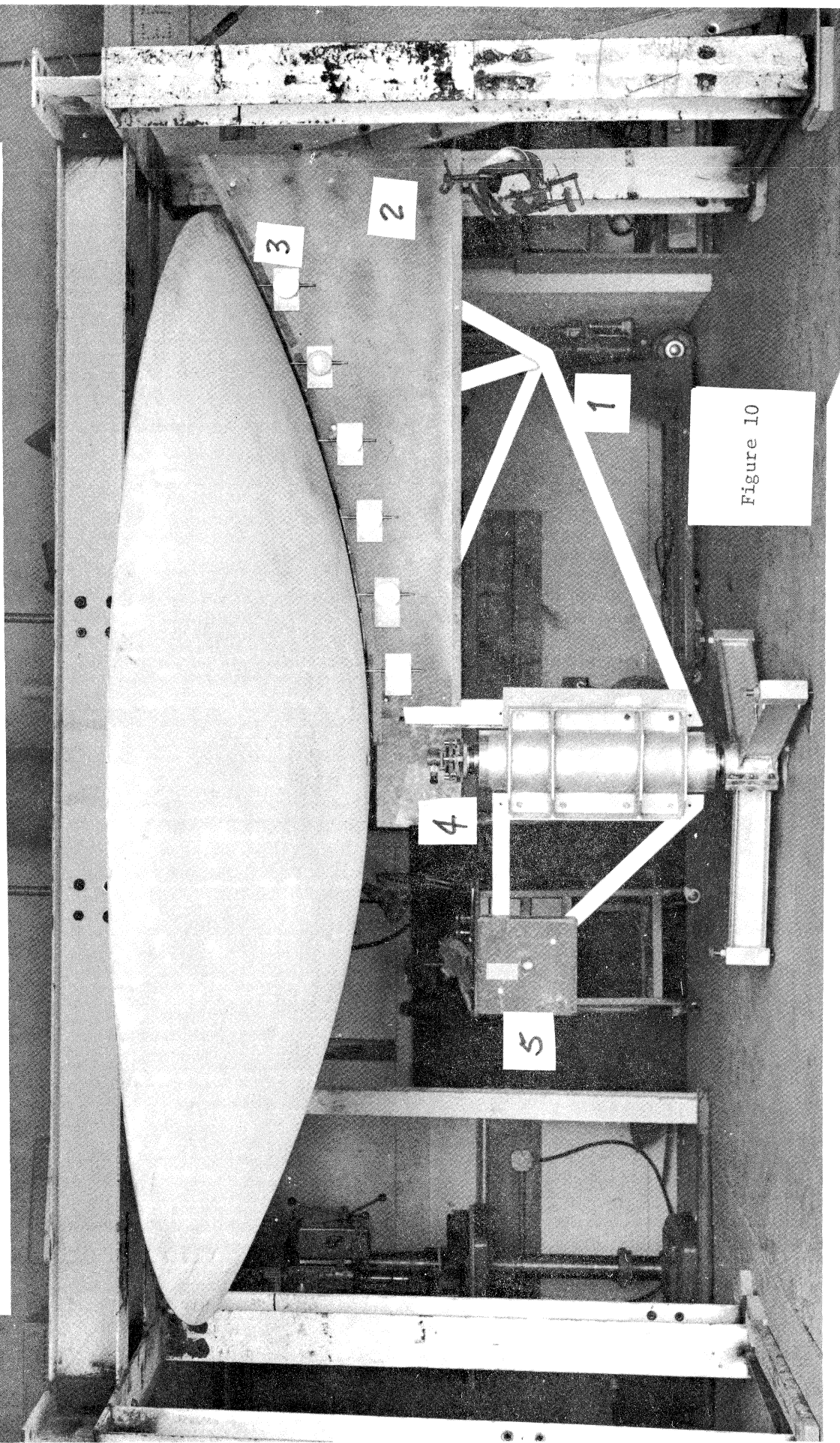


Figure 10

### Measurement of template no. 1 (Green Bank, March, 1977)

Avg. profile error =  $3.8 \times 10^{-3}$  in. rms

$$= 0.097 \text{ mm rms}$$

A2:35.75 A1:38.30 A3:40.75 A4:42.90

in. Location of actuators

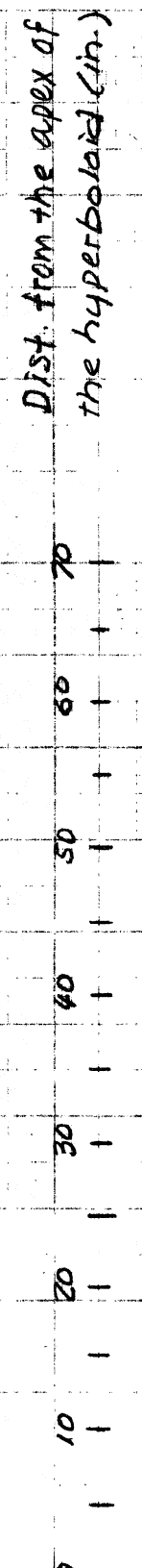
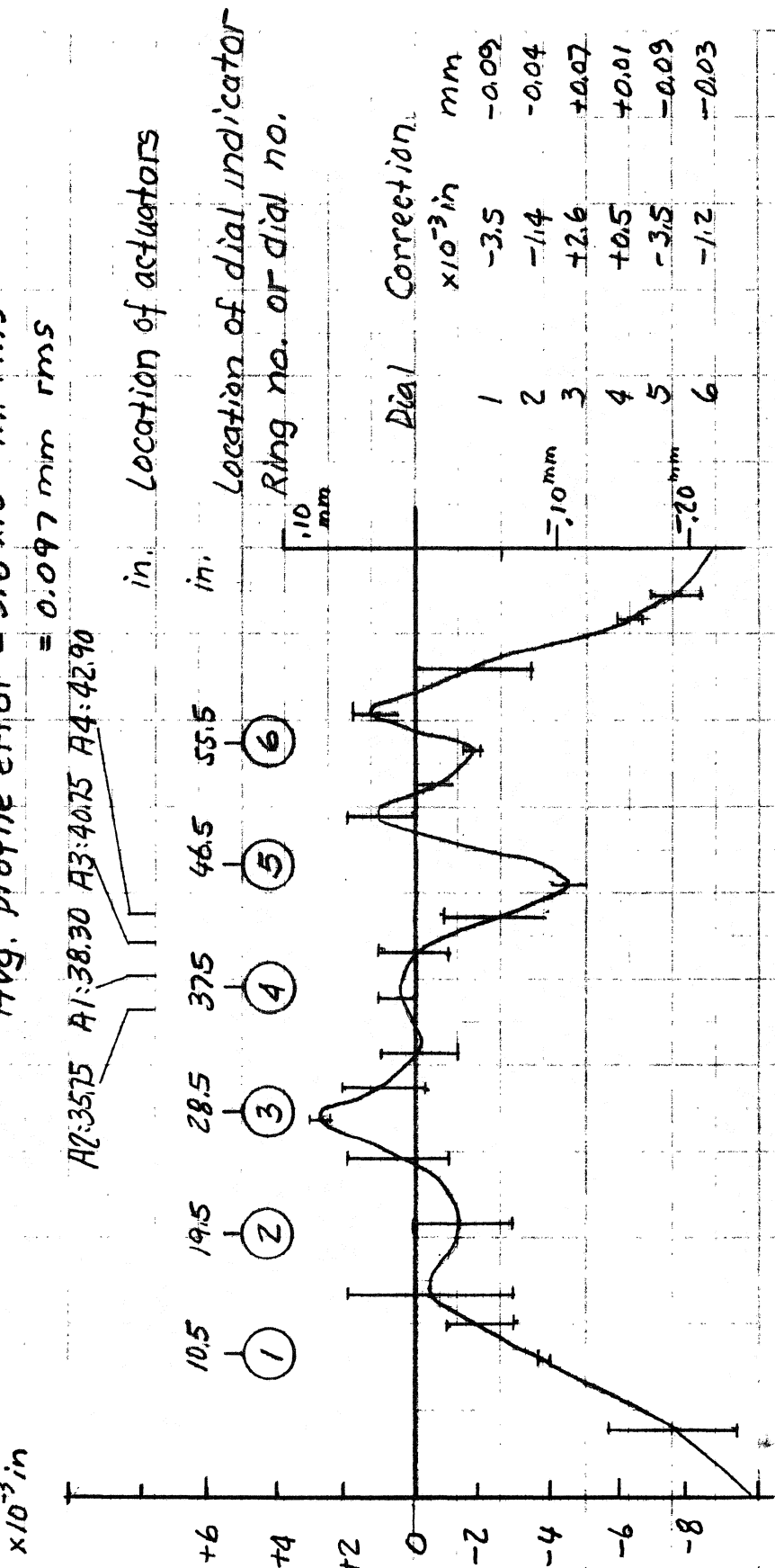
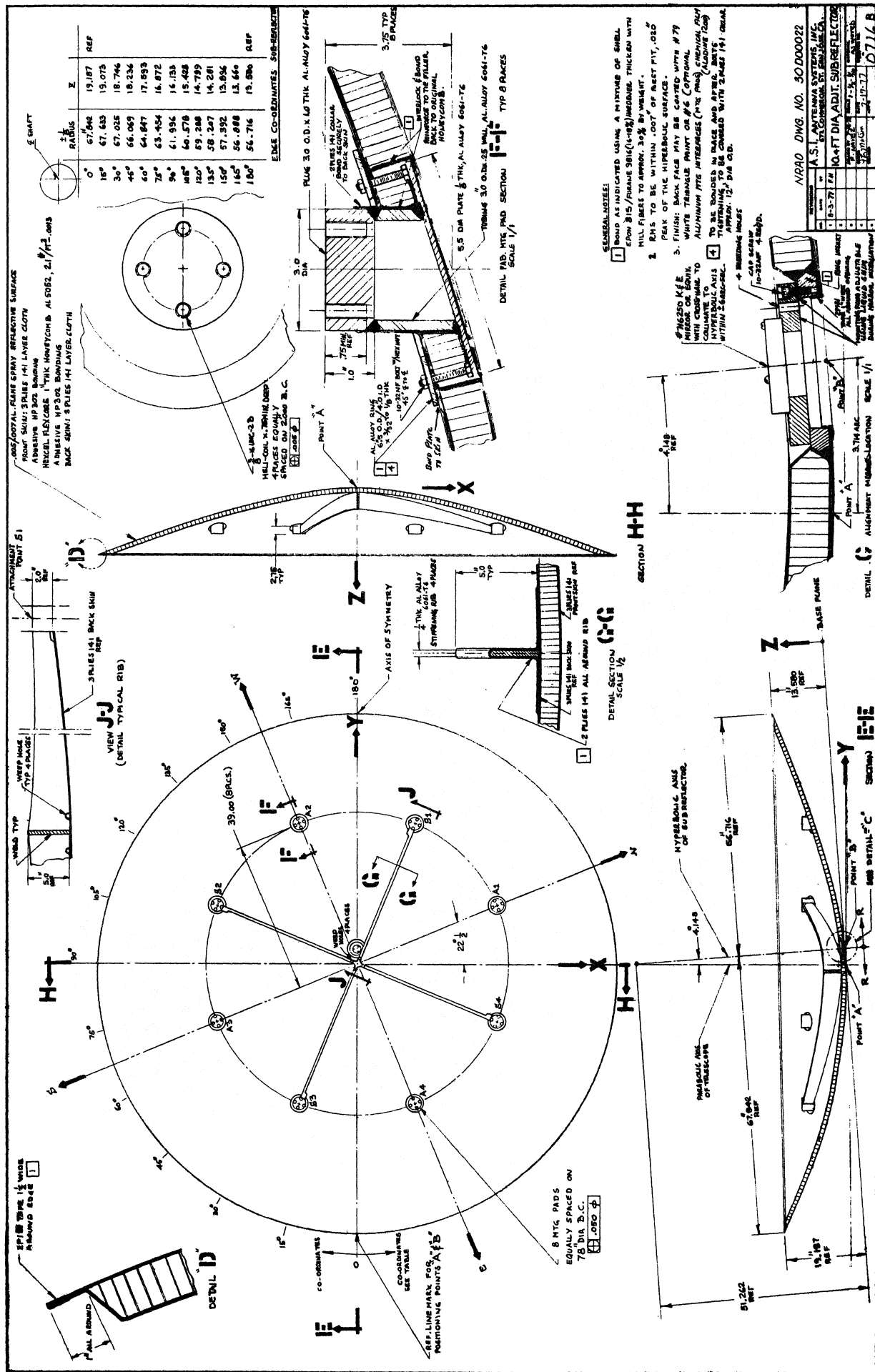


Figure 11 The error on the profile and the reference system of the template used in the measurement.

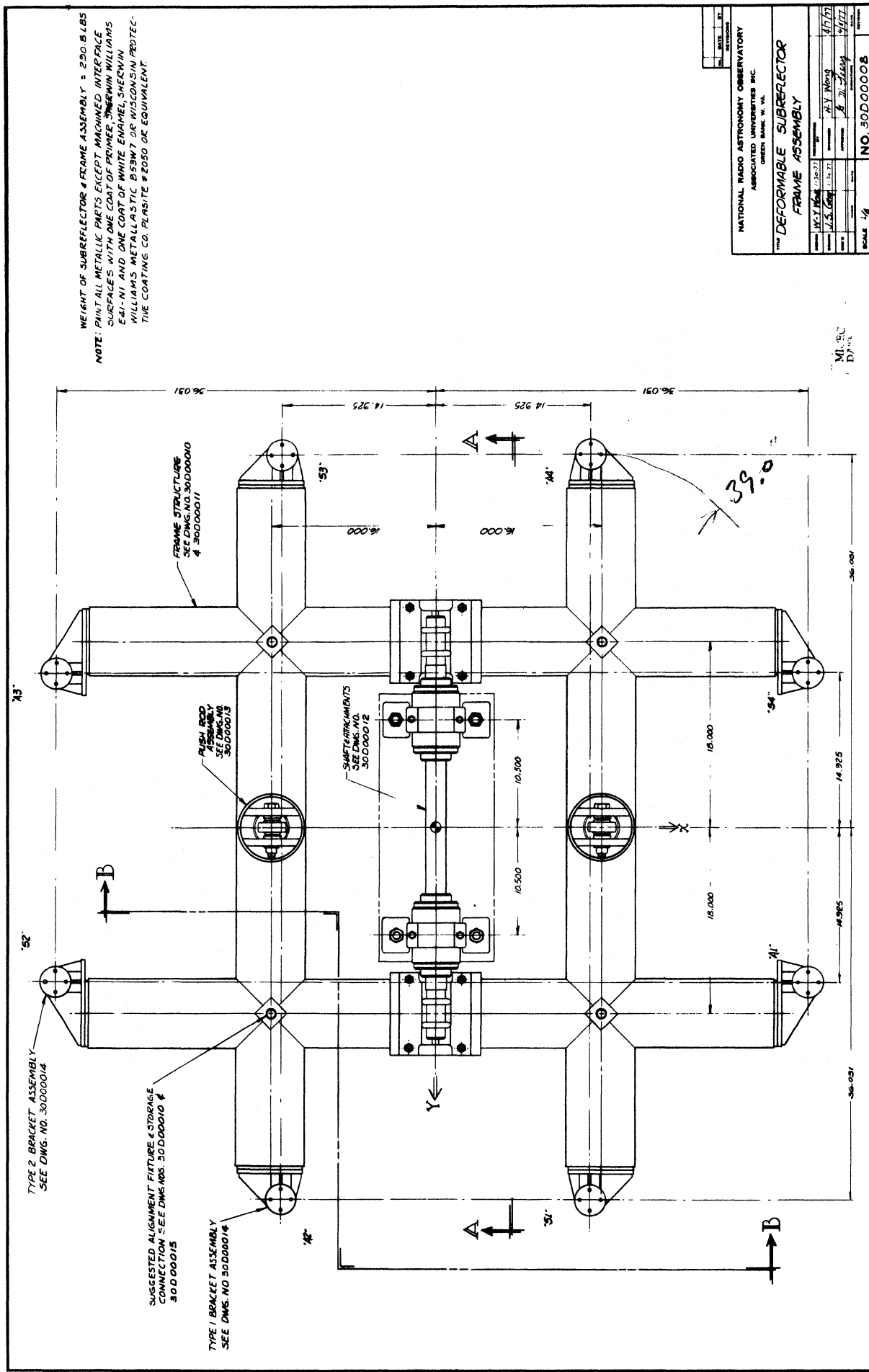
## APPENDIX A

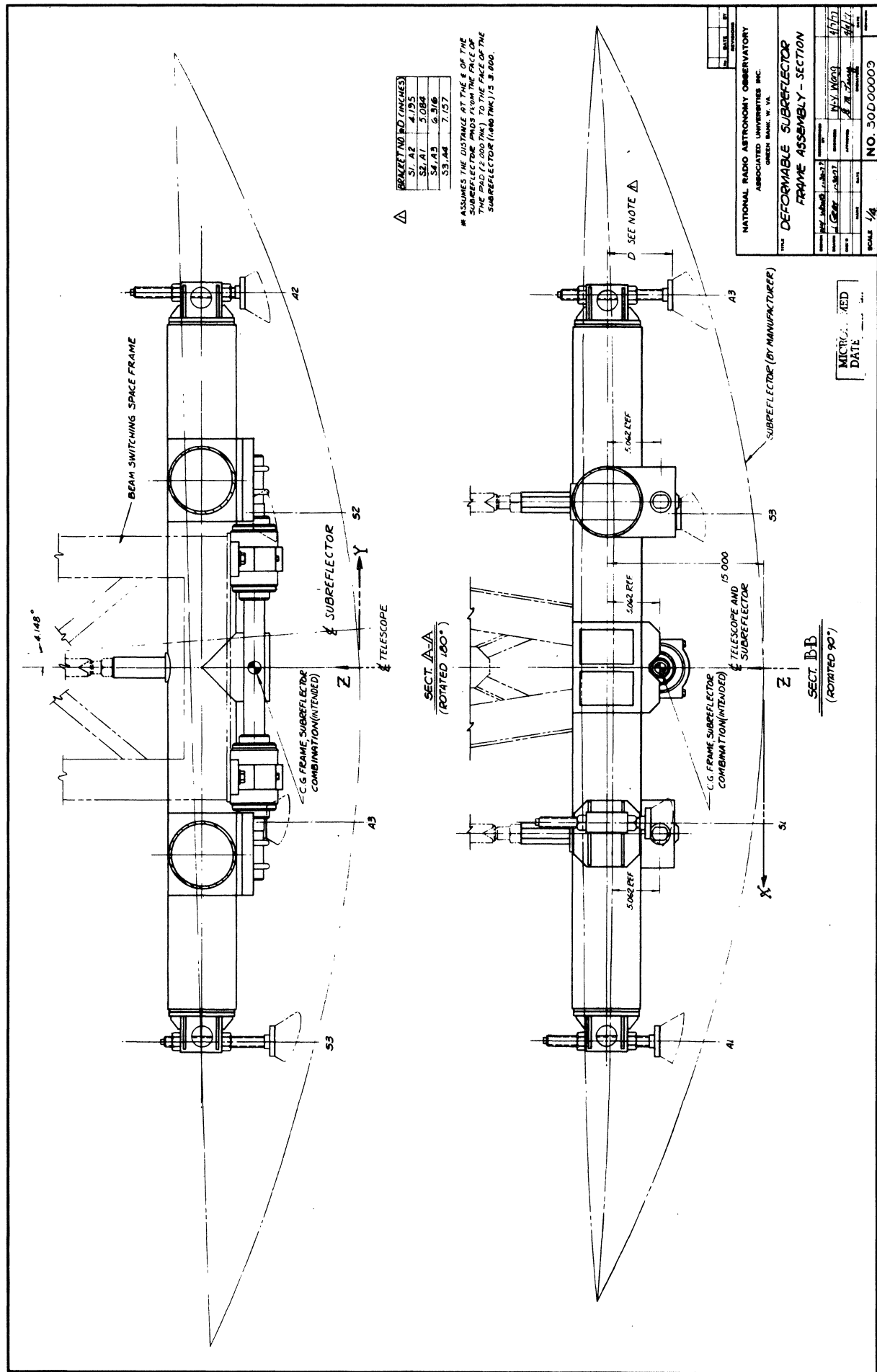
Engineering drawing of the Subreflector Surface



APPENDIX B

Engineering drawings of the Bakc-up Frame DWG No. 30 D 00008  
to 30 D 00016.



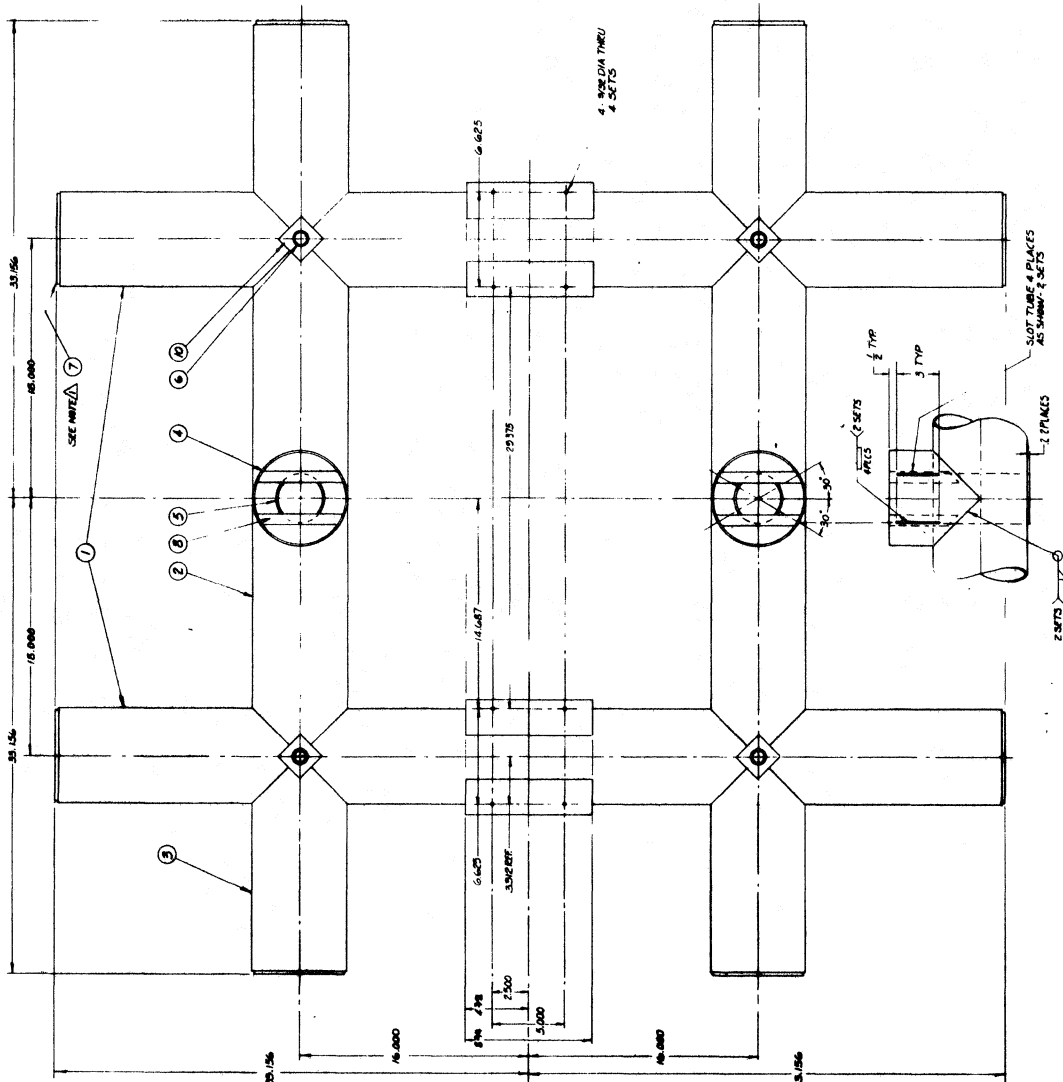


LIST OF MATERIAL		
ITEM	QTY	DESCRIPTION
1	2	PIPE 6' X 1/2" SCH 40 SDR 30
2	2	PIPE 6' X 1/2" SCH 40 SDR 30
3	4	PIPE 6' X 1/2" SCH 40 SDR 30
4	2	PIPE 5 SCH 40 PIPE 6' X 1/2" SDR 30
5	3	PIPE 6' X 1/2" SCH 40 PIPE 6' X 1/2" SDR 30
6	4	PLUGS 1/2" SDR 30
7	15	PLUGS 1/2" SDR 30
8	4	BRACKET 3/4" THK 1/2" WIDG
9	10	PIR 1/2" TJK - 2 1/4" X 2 1/4"
10	8	PIR 1/2" TJK - 3 1/4" X 2 1/4"
11	12	GUSSET 3/4" THK 1/2" WIDG

**NOTE 5:**

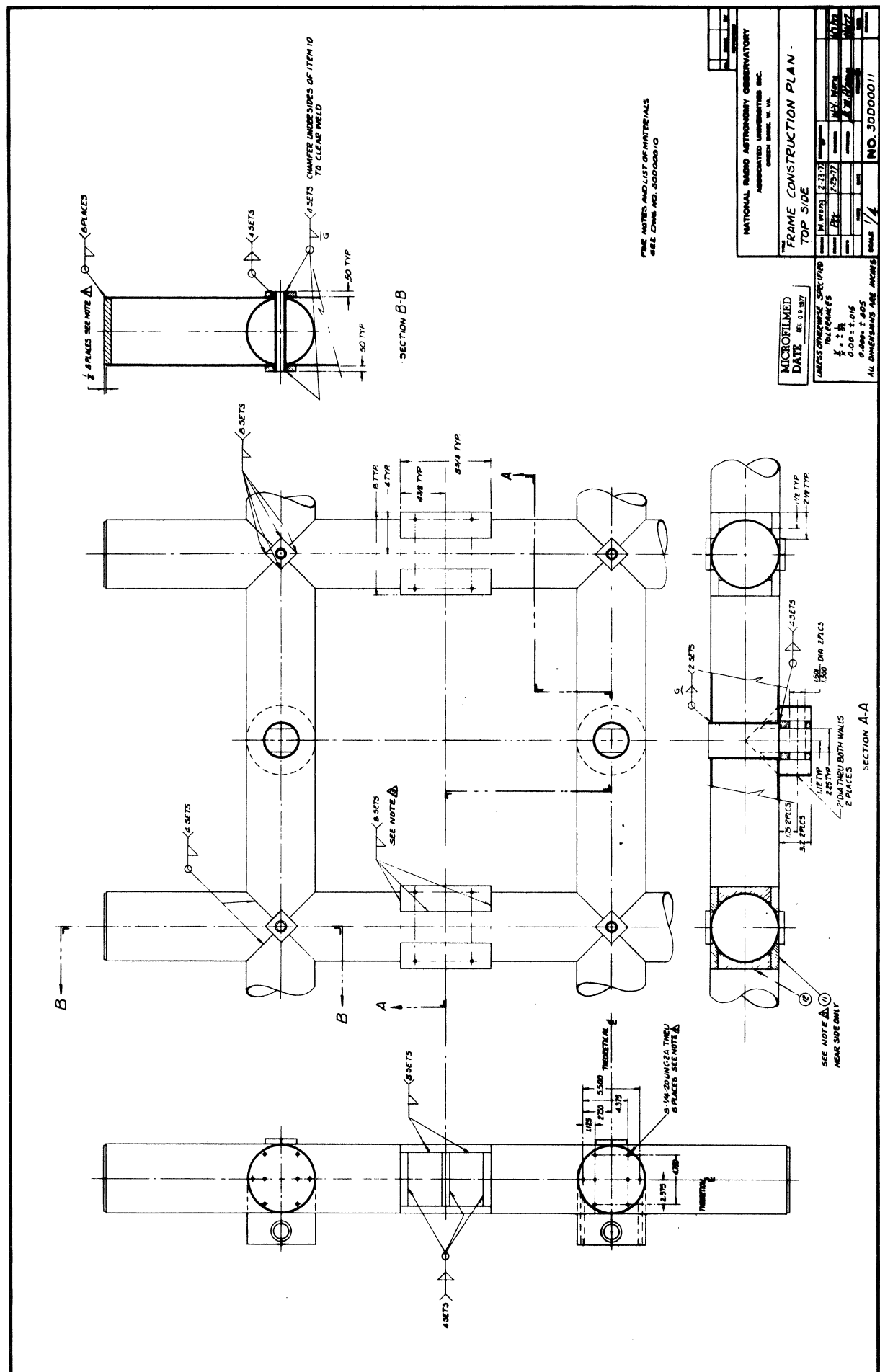
FRAME TO BE WELDED CONSTRUCTION THROUGH.  
CENTER LINES OF ALL G PIPE TO BE IN THE SAME  
HORIZONTAL PLANE & PERPENDICULAR TO EACH  
OTHER AT ALL INTERSECTIONS.

OUT UNLESS OTHER METHODS OF ASSEMBLY ARE  
DETAILED. ALL WELDS TO BE CONTINUOUS FOR  
ENTIRE LENGTH OF ATTACHMENT (MATCHING)  
SURFACES.

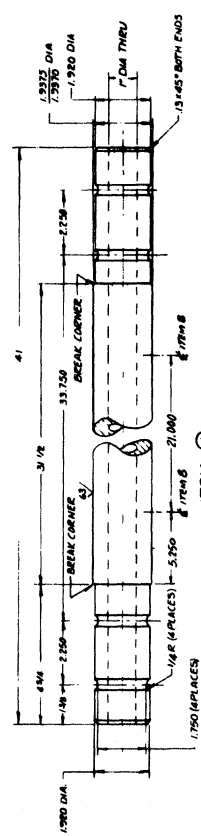


NATIONAL RADIO ASTRONOMY OBSERVATORY UNIVERSITY OF VIRGINIA INC. CHARLOTTESVILLE, VA.	
FRAME CONSTRUCTION PLAN - <b>BOTTOM SIDE</b>	
MATERIALS	ITEM NO. (WING 1-3317)
STRUCTURE SPECIFIED	ITEM NO. (WING 1-3317)
TELEGRAMS	ITEM NO. (WING 1-3317)
$\frac{1}{2} \times 10$	ITEM NO. (WING 1-3317)
0.00 x 1.06	ITEM NO. (WING 1-3317)
0.00 x 1.06	ITEM NO. (WING 1-3317)
ALL CONSTRUCTIONS ARE IN INCHES	
NO. 30/20010	

**MICROFILMED**  
**DATE** 09-09-97

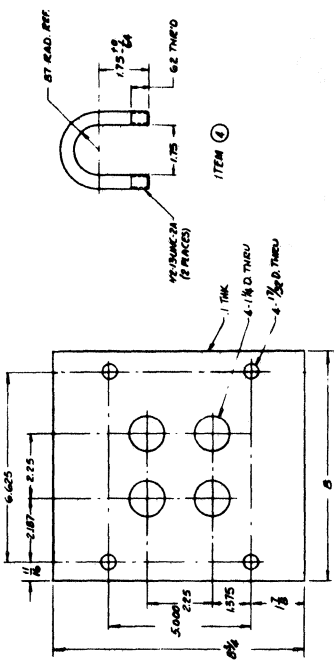
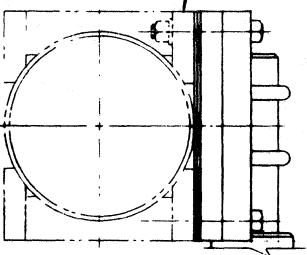


MATERIAL LIST		REMARKS
ITEM	DESCRIPTION	QUANTITY
1.	SHARP TOED STEEL CHARGE PLATE	1
2.	BLOCK GOG-1 TO ALUM. BURNER	1/2
3.	SHIM PACK. TO LINE LAMINATES AND THE ALUM. SHEETS	1
4.	WRENCH VIBRA STATION 353 STREET	1
5.	HOE NO. 10 FOR DUSTING 2A 1/12	1
6.	LOCATING SHEET 1/4 IN.	1
7.	MIC. ANFT. NO. 13/16 2B	1
8.	DRILL CHARD. 1/16 INCH SHAPED DRILL	1



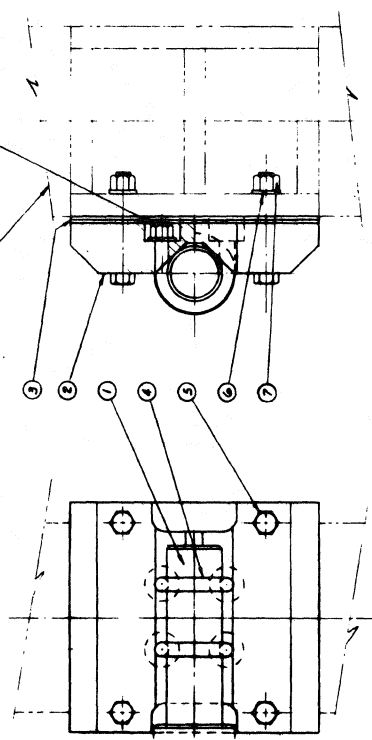
卷之三

ITEM ①

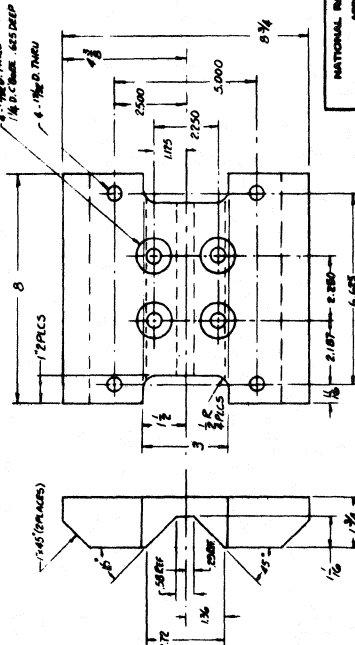


SEE DWS NOS. 300000/D & 300001/  
FOR FRAME CONSTRUCTION

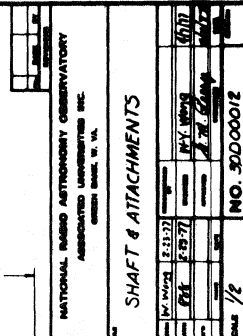
**IF NO SHIMS (ITEM 9) ARE REQUIRED  
ENDS OF U-BOLT (ITEM 4) MUST NOT  
PROJECT BEYOND SURFACE OF ITEM 2**



3



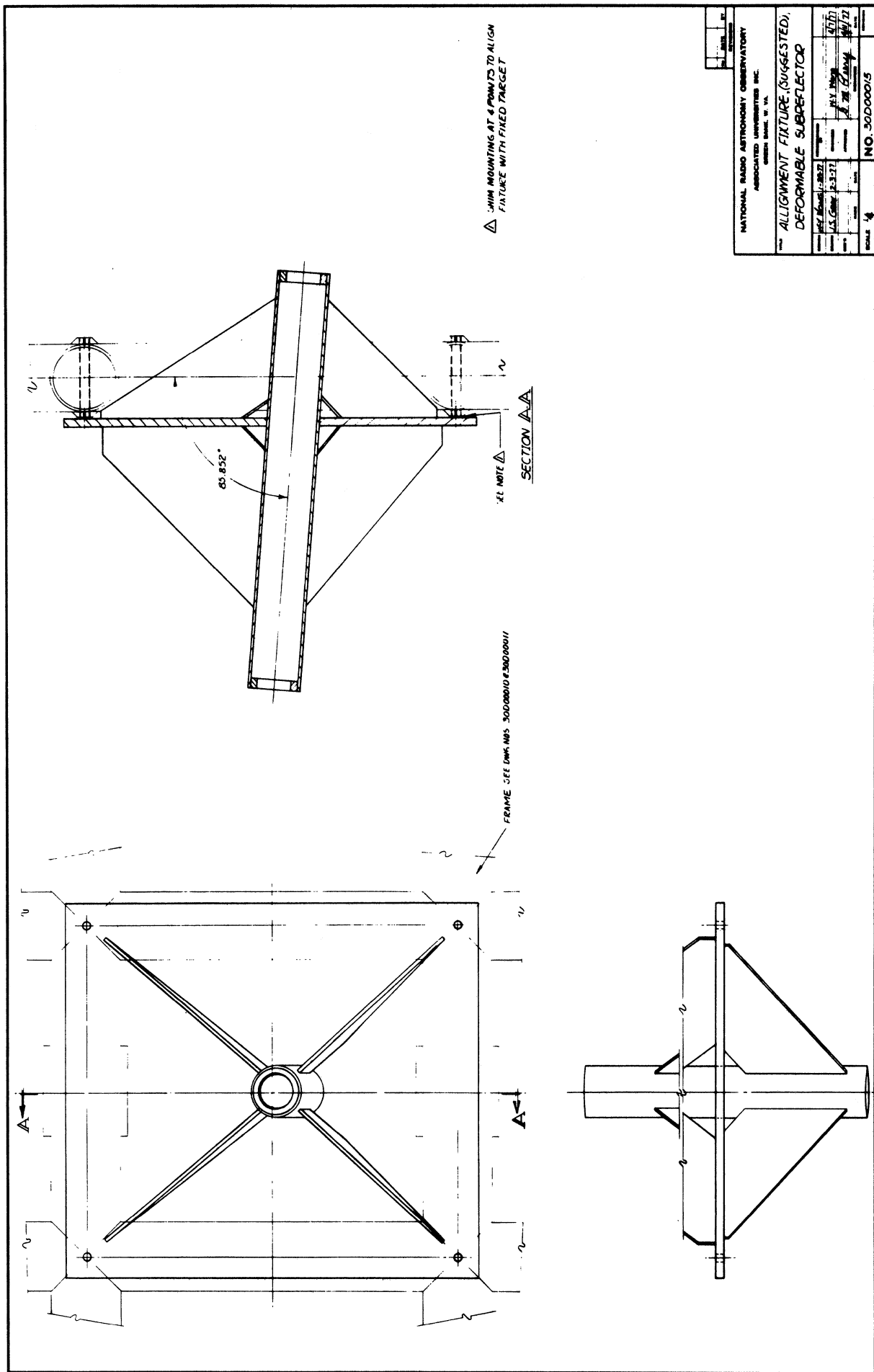
**MICROFILMED**  
**DATE** 01-03-1977

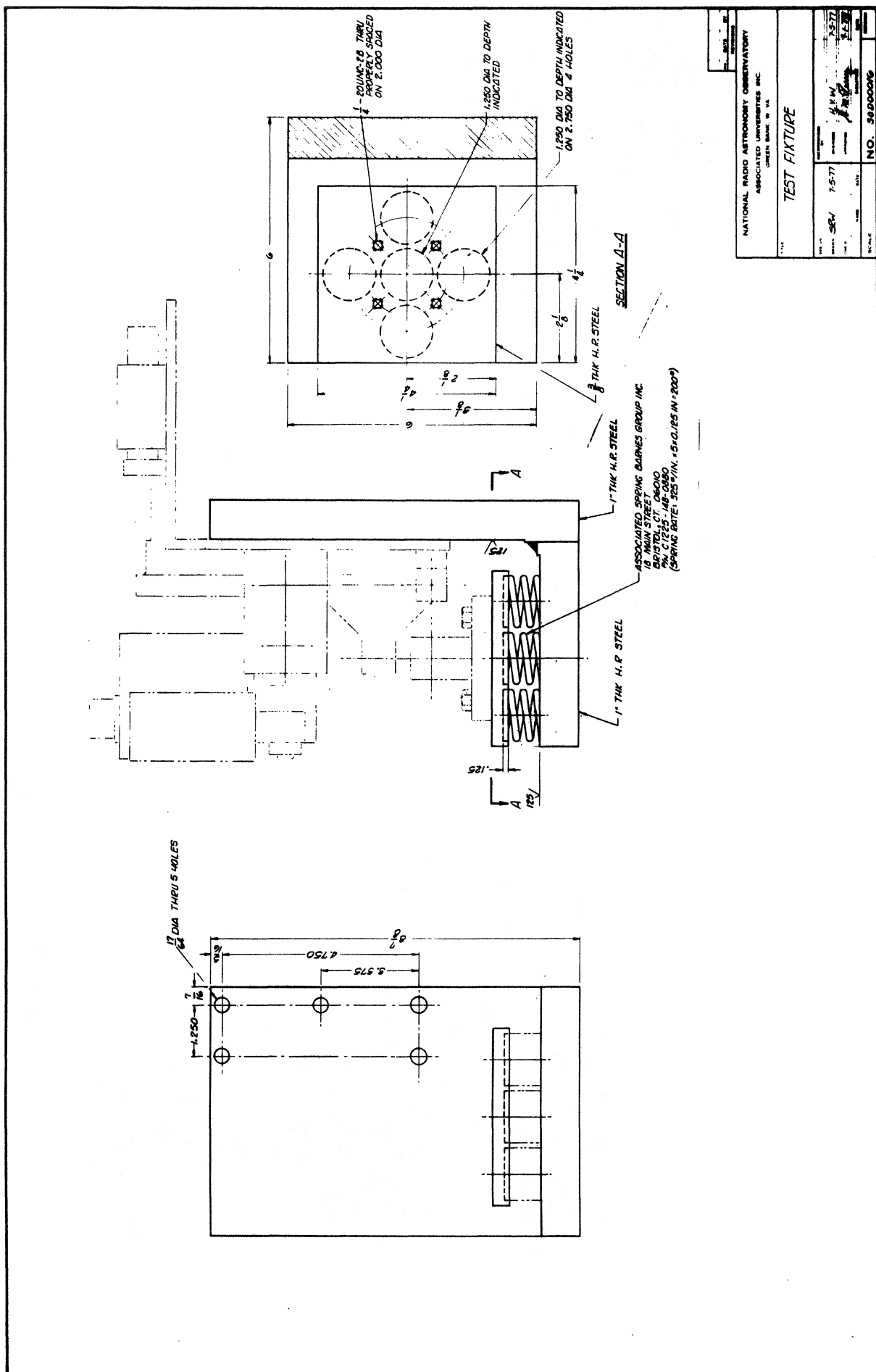


**MICROFILMED**  
**DATE** 01-03-1977



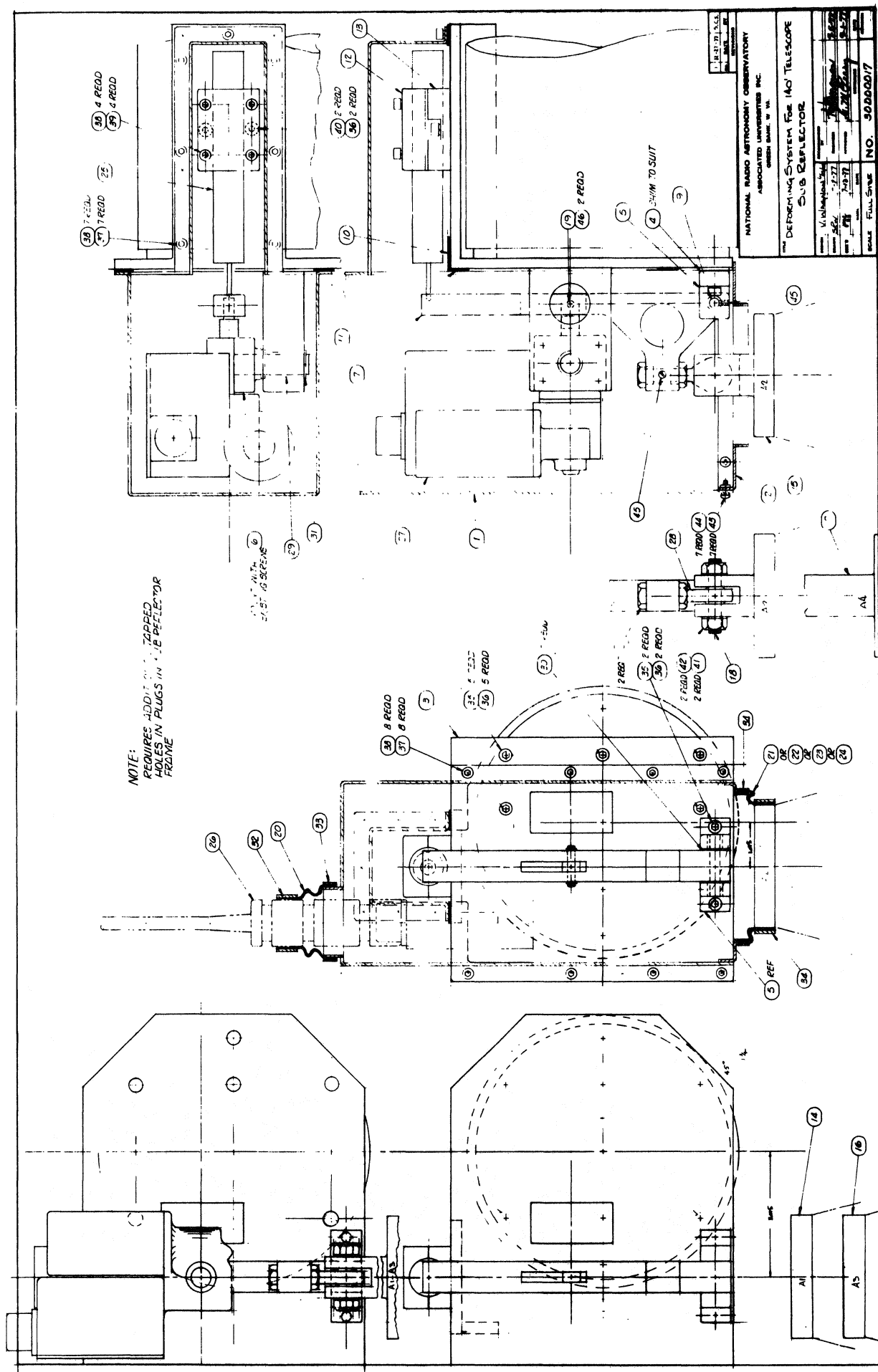


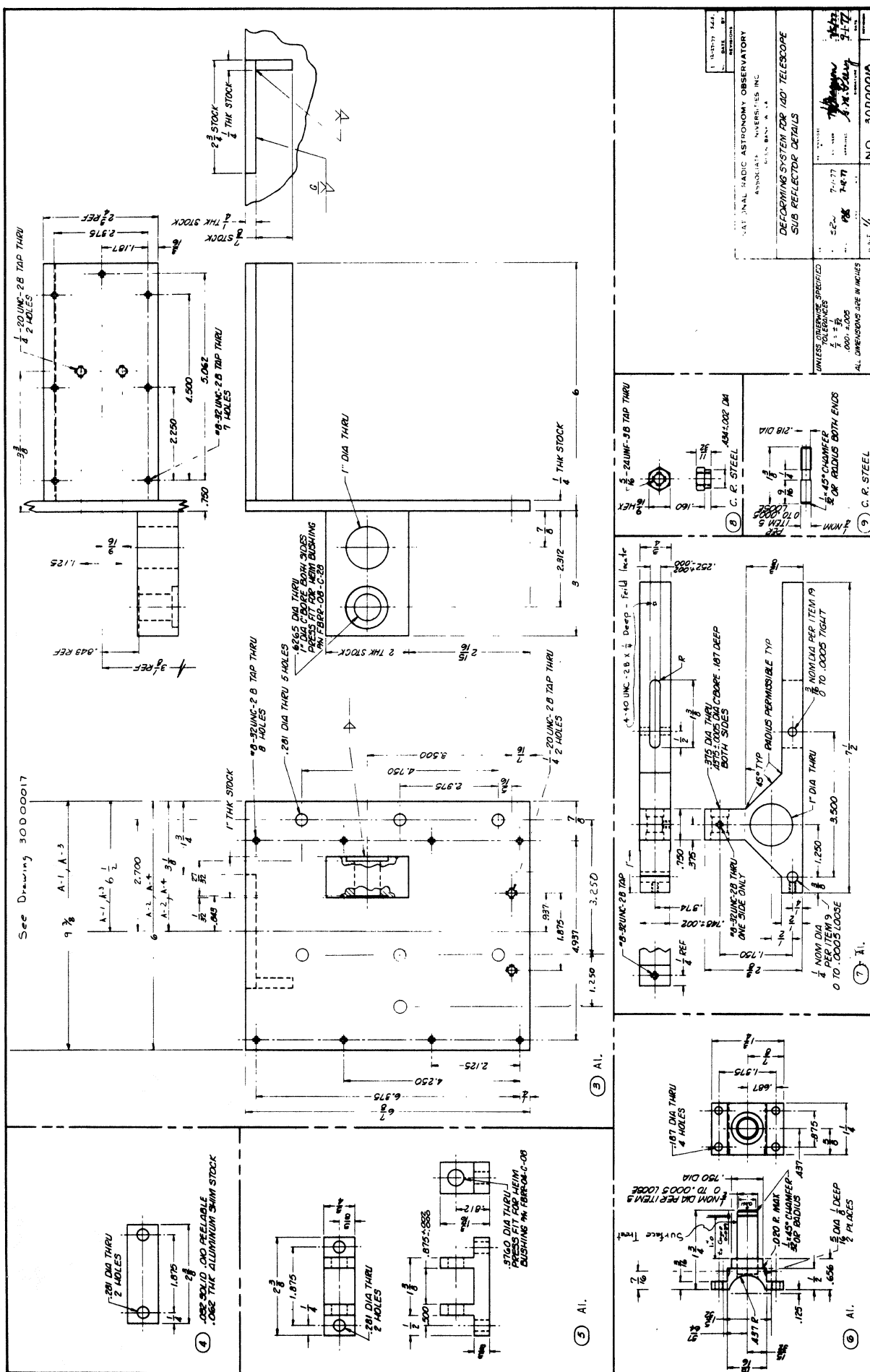




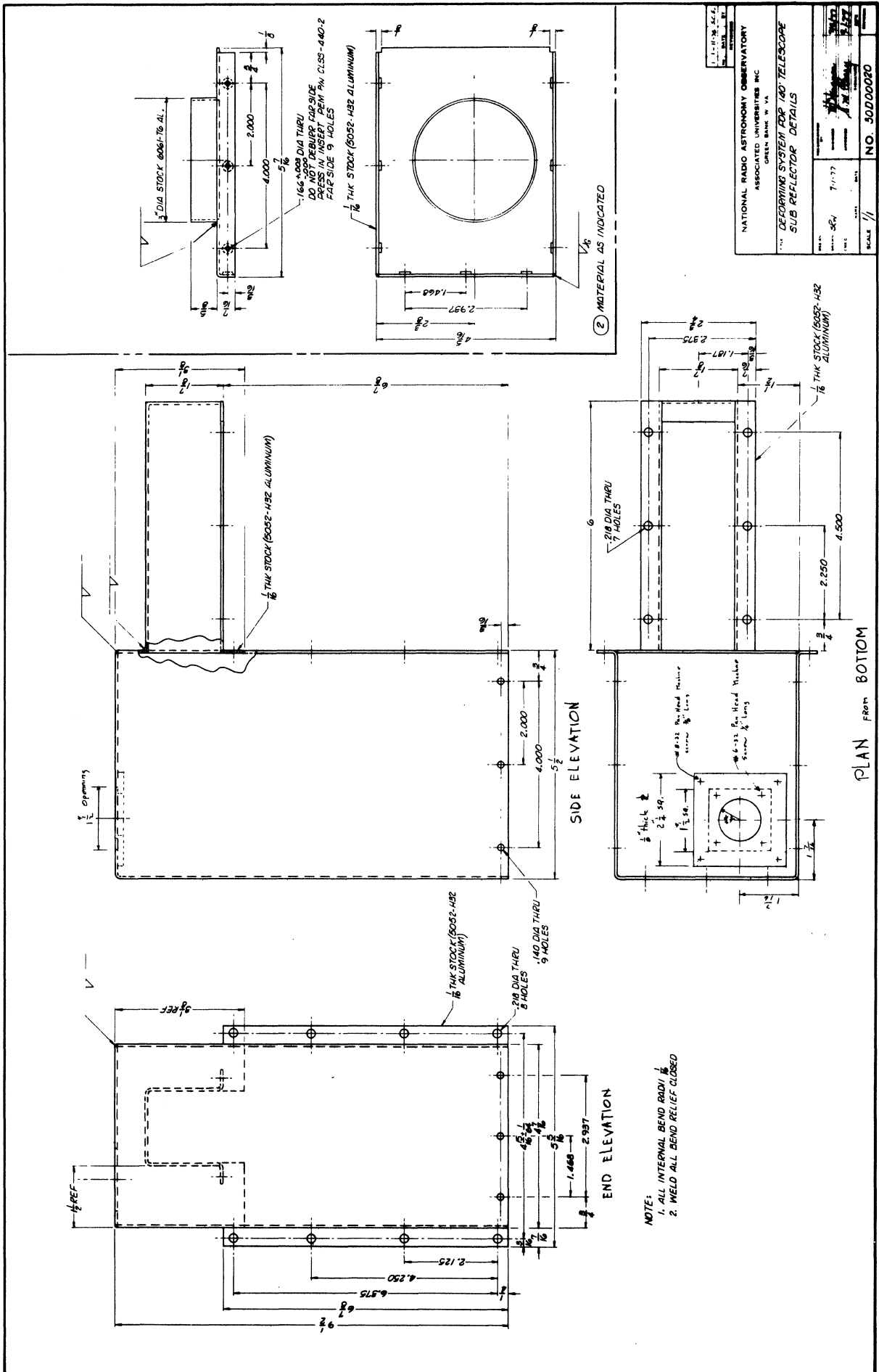
APPENDIX C

Engineering Drawings of the Deforming System DWG No. 30 D 00017  
to 30 D 00020.



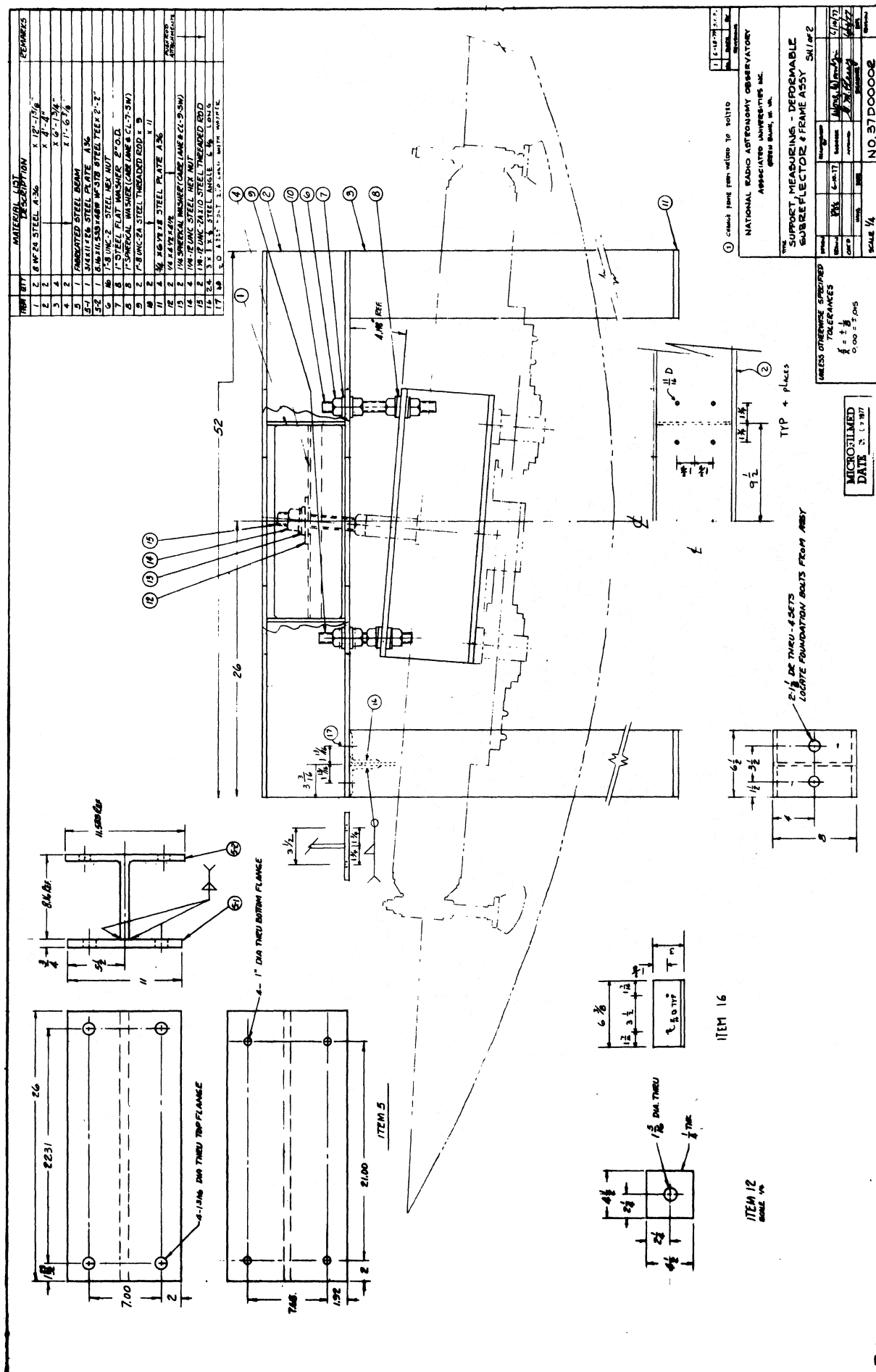


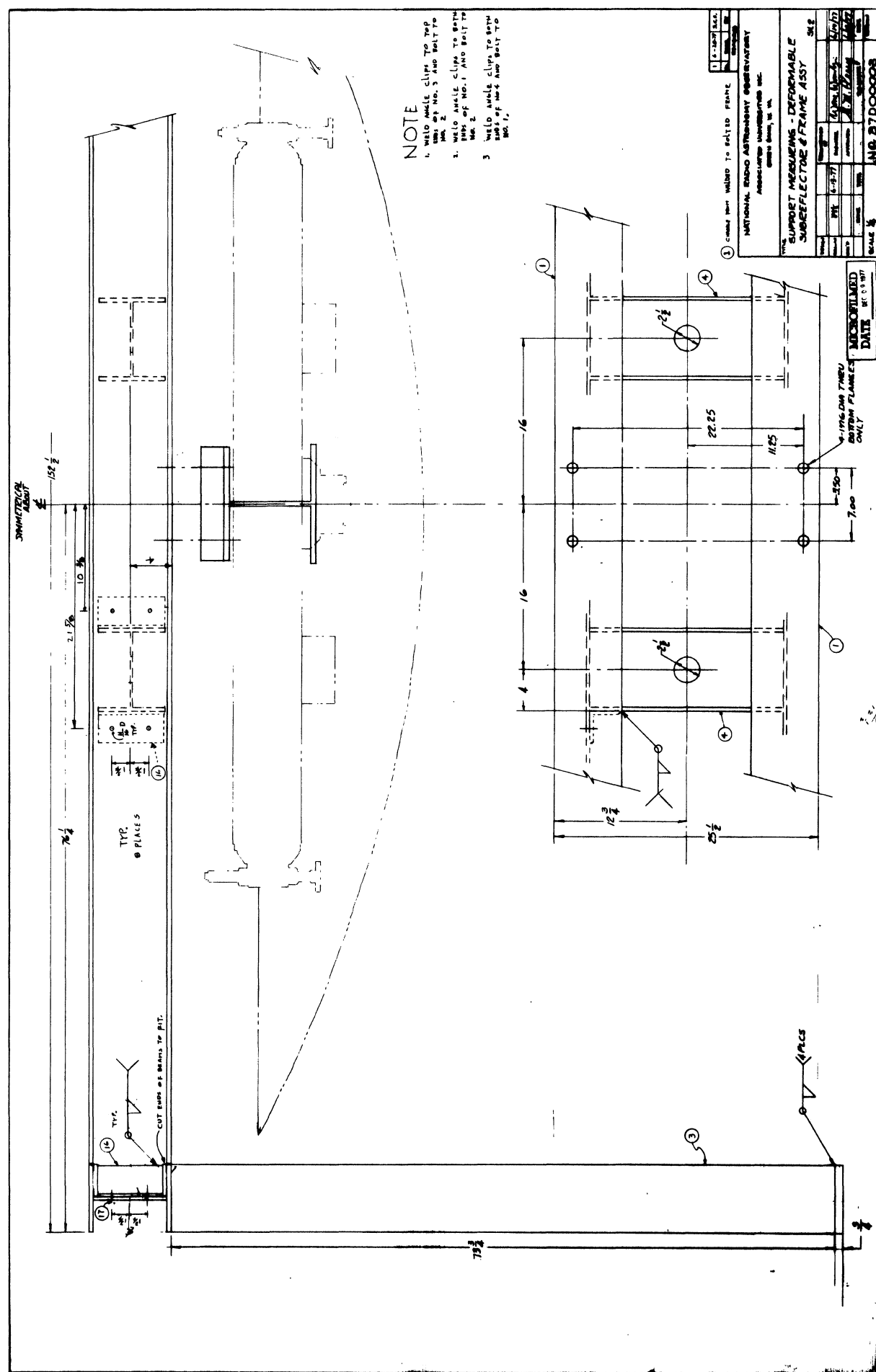




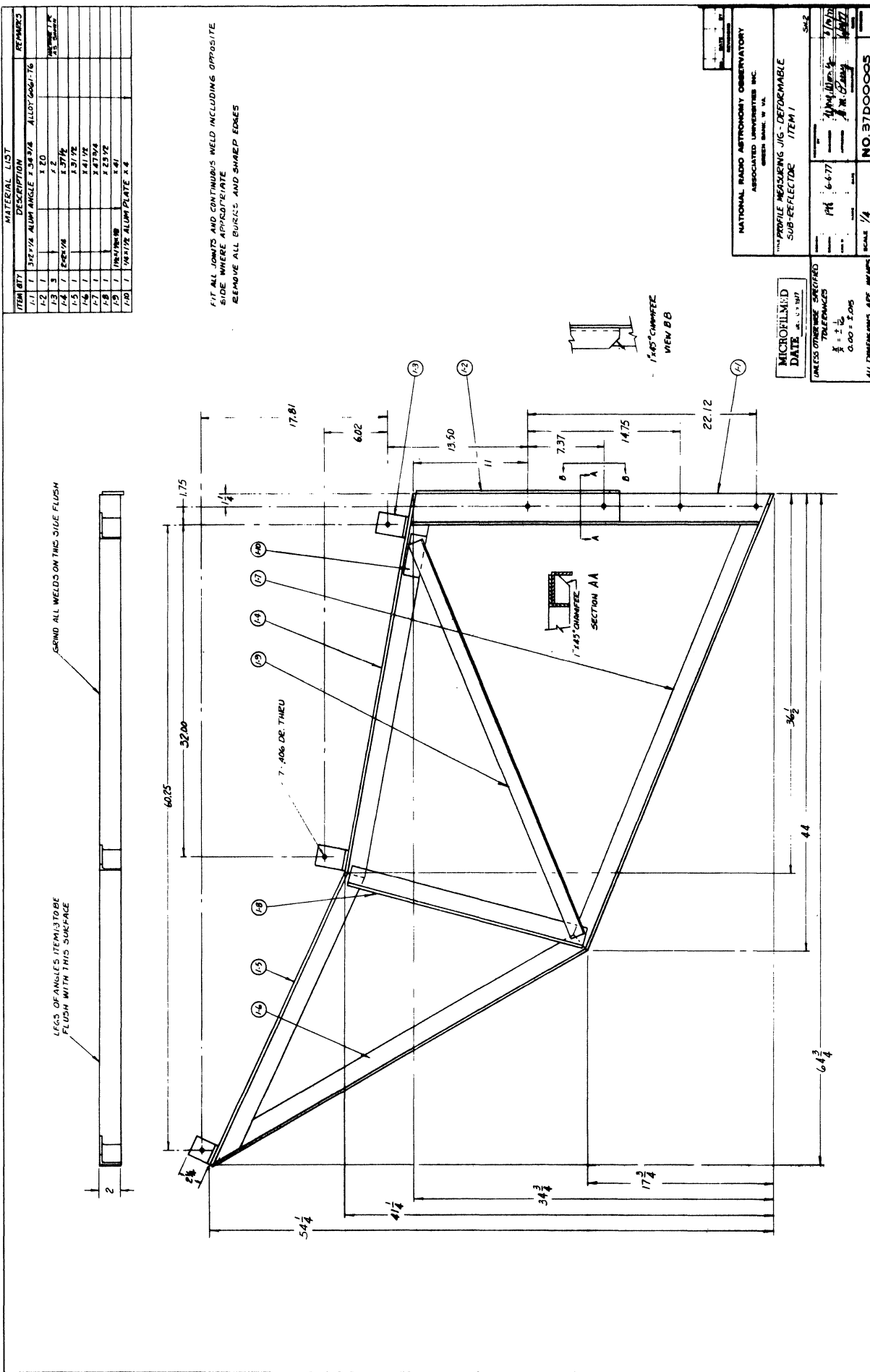
APPENDIX D

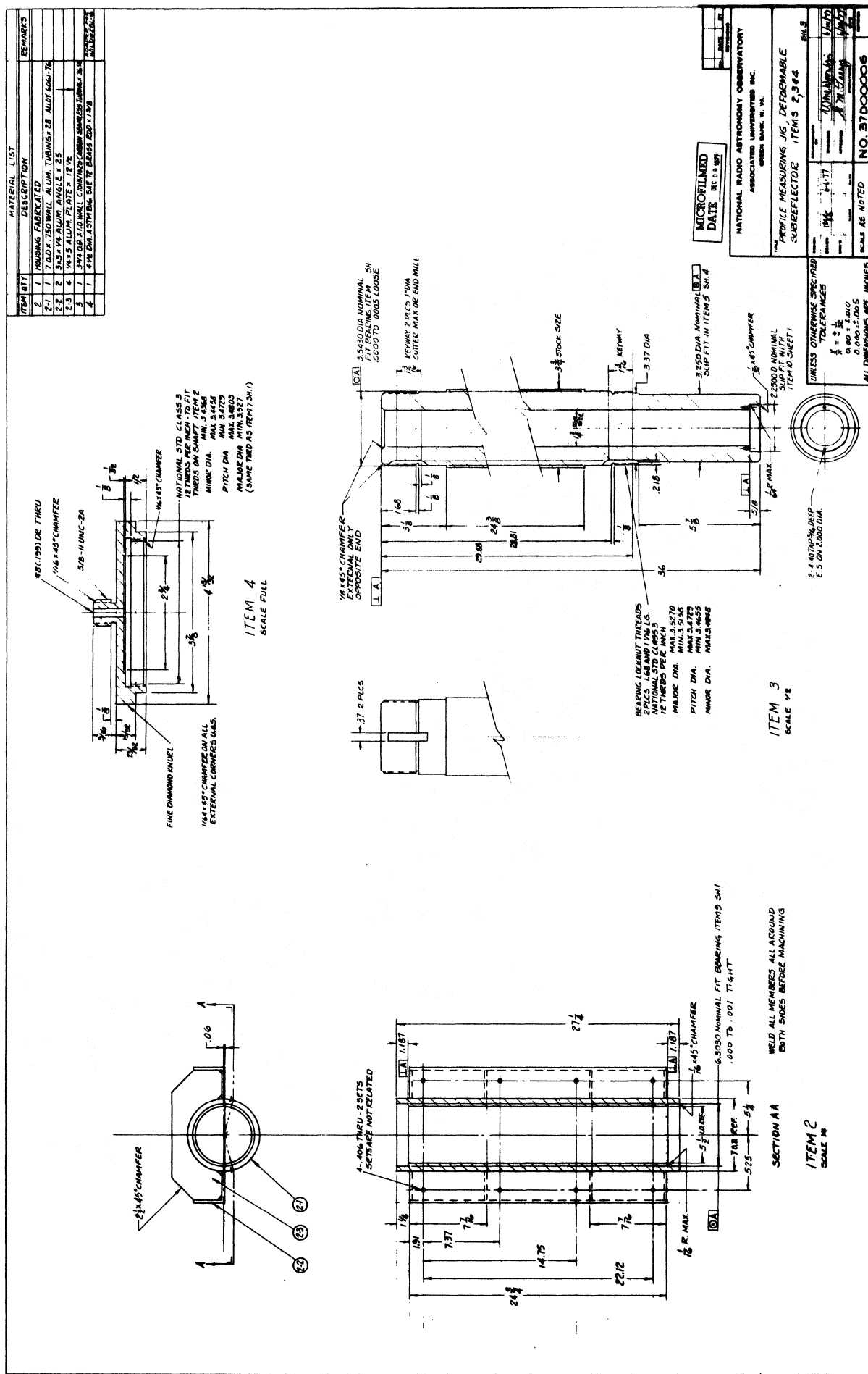
Engineering Drawings of the Measuring Jig and the Gentry DWG No.  
37 D 00002 to 37 D 00007.













## APPENDIX E

The Best Fitting of a Hyperboloid

The equation of the hyperboloid described in eq. (1) is repeat here:

$$z_0 = (c - \frac{1}{2}a) \left\{ \sqrt{1 + \frac{r^2}{bc}} - 1 \right\} \quad (1)$$

where  $r^2 = x^2 + y^2$ , and the coordinate system illustrated in figure 1.

The subreflector is small in size and stiff in a sense that the defocusing type of deformation is considered neglegible. Hence, as a rigid body motion, the five degree of freedom are:

- $\Delta X$ : translation in X direction
  - $\Delta Y$ : translation in Y direction
  - $\Delta Z$ : translation in Z direction
  - $\Delta \phi$ : rotation about the X axis, where  $Z=Y\Delta\phi$
  - $\Delta \psi$ : rotation about the Y axis, where  $Z=X\Delta\psi$
- (2)

with small amount of motions, eq. (1) can be written as:

$$z_i = (c - \frac{1}{2}a) \left\{ \sqrt{1 + \frac{(x_i - \Delta x)^2 + (y_i - \Delta y)^2}{bc}} - 1 \right\} + \Delta z + y_i \Delta \phi + x_i \Delta \psi \quad (3)$$

in which, without losing the accuracy, the mathematics is simplified by letting

$$\begin{aligned} (x_i - \Delta x)^2 &= x_i^2 - 2x_i \Delta x \\ (y_i - \Delta y)^2 &= y_i^2 - 2y_i \Delta y \end{aligned} \quad (4)$$

so the eq. (3) became

$$z_i = \left( c - \frac{1}{2}a \right) \left\{ \sqrt{1 + \frac{x_i^2 + y_i^2}{bc}} - 2 \frac{x_i \Delta x + y_i \Delta y}{bc} - 1 \right\} + \Delta z + y_i \Delta \phi + x_i \Delta \psi \quad (5)$$

Call

$$A = 1 + \frac{x_i^2 + y_i^2}{bc}, \quad \varepsilon = -2 \frac{x_i \Delta x + y_i \Delta y}{bc} \quad (6)$$

with a general expression that

$$\sqrt{A + \varepsilon} = \sqrt{A} \cdot \sqrt{1 + \frac{\varepsilon}{A}} = \sqrt{A} \left( 1 + \frac{1}{2} \frac{\varepsilon}{A} \right) = \sqrt{A} + \frac{\varepsilon}{2\sqrt{A}} \quad (7)$$

combining (6) and (7)

$$\sqrt{A + \varepsilon} = \sqrt{1 + \frac{r_i^2}{bc}} - \frac{1}{\sqrt{1 + \frac{r_i^2}{bc}}} \cdot \frac{x_i \Delta x + y_i \Delta y}{bc} \quad (8)$$

substituting (8) to (5)

$$z_i = \left( c - \frac{1}{2}a \right) \left\{ \sqrt{1 + \frac{r_i^2}{bc}} - \frac{1}{\sqrt{1 + \frac{r_i^2}{bc}}} \cdot \frac{x_i \Delta x + y_i \Delta y}{bc} - 1 \right\} + \Delta z + y_i \Delta \phi + x_i \Delta \psi \quad (9)$$

Call

$$U = \left( c - \frac{1}{2}a \right), \quad T = \left( c - \frac{1}{2}a \right) \frac{1}{bc}, \quad R_i = \sqrt{A}$$

Eq. (9) becomes

$$z_i = UR_i - \frac{T}{R_i} (x_i \Delta x + y_i \Delta y) - U + \Delta z + y_i \Delta \phi + x_i \Delta \psi \quad (10)$$

Equation (10) can be rewritten as

$$\Delta z - \frac{\nabla x_i}{R_i} \Delta x - \frac{\nabla y_i}{R_i} \Delta y + y_i \Delta \phi + x_i \Delta \psi = z_i - \bar{U} R_i + \bar{V} \quad (11)$$

Call

$$[F] = \begin{bmatrix} 1 & -\frac{\nabla x_1}{R_1} & -\frac{\nabla y_1}{R_1} & +y_1 & +x_1 \\ & \vdots & \vdots & & \\ & & \vdots & & \\ & & & & \\ 1 & -\frac{\nabla x_n}{R_n} & -\frac{\nabla y_n}{R_n} & +y_n & +x_n \end{bmatrix}_{n \times 5}$$

$$[G] = \begin{bmatrix} \Delta z \\ \Delta x \\ \Delta y \\ \Delta \phi \\ \Delta \psi \end{bmatrix}_{5 \times 1}$$

and the deviation from the design [H] is

$$[H] = \begin{bmatrix} z_1 - \bar{U} R_1 + \bar{V} \\ \vdots \\ z_n - \bar{U} R_n + \bar{V} \end{bmatrix}_{n \times 1}$$

So that eq. (11) is written as

$$[F][G] = [H] \quad (12)$$

Premultiplying the transpose of [F] to both sides of (12):

$$[F]^T [F][G] = [F]^T [H] \quad (13)$$

where

$$[\alpha] = [F]^T [F]$$

and the unknown [G] is solved,

$$[G] = [\alpha]^{-1} [F]^T [H] \quad (14)$$

The computer program listing, sample input and the result are also included.

```

C C BEST FIT FOR HYPERBOLOID WITH 5 DOF
C C DEC. 12,1977 A4=-.100, A-2=-.100,A-1=+.100,A-3=+.100
C C DIMENSION A(144,5),B(144)*AA(5,5)*BB(5),S(5),C(144)
C X, X(144),Y(144),Z(144),STM(72),R(144),R0(6)
C X, RAD(6),LL(5),MM(5),LBF(144),DEV(144)
C X, ADJ(6)

C C INITIATION
C C DATA RADI / 266.7, 495.3, 723.9, 952.5, 1181.1, 1409.7 /
C C DATA AA, BB, S / 25*0., 5*0., 5*0. /
C C DATA ADJ / -.09, -.04, .07, .01, -.39, -.03 /
C C J1=214.185*25.4
C C 2=24585.8338*25.4
C C 3=C1/C2

C C X(I), Y(I)
C C K=0
C C PH=0.
C C ANG=15.*3.1416/180.
C C DO 60 I=1,24
C C COSP=COS(PH)
C C SINP=SIN(PH)
C C DO 50 J=1,6
C C K=K+1
C C X(K)=RADI(J)*COSP
C C Y(K)=RADI(J)*SINP
C C 50 CONTINUE
C C PH=PH+ANG
C C 60 CONTINUE

C C INPUT : STATEMENT & GAP READINGS
C C READ(5,900) (STM(I),I=1,72)
C C PRINT 914, (STM(I),I=1,72)
C C READ(5,901) (ROL(I),I=1,6)
C C DO 70 I=1,6
C C R0(I)=R0(I)+ADJ(I)
C C 70 CONTINUE

C C Z(I)
C C K=0
C C AG=0.
C C DO 200 I=1,24
C C DO 100 J=1,6
C C K=K+1
C C READ(5,917) R(K)
C C C(K)=SQR T(1.+(X(K)*X(K)+Y(K)*Y(K))/C2)
C C Z(K)=C1*(C(K)-1.)*R0(J)-R(K)
C C AG=AC+R0(J)-R(K)
C C 100 CONTINUE
C C 200 CONTINUE
C C AG=AG/144.

```

FORTRAN IV G LEVEL 20 MAIN DATE = 17346 PAGE 0002  
 15/14/52

```

0039      C PRINT 916,(R(I),I=1,144)
          C PRINT X,Y,Z & AVG. GAP
          C PRINT 902,(I,X(I),Y(I),Z(I),I=1,144)
          C PRINT 903,AG
          C BEST FIT BY PARALLEL SHIFT
          C
          SUM=0.
          DO 250 I=1,144
          ZBF(I)=C1*(C(I)-1.)*AG
          DEV(I)=Z(I)-ZBF(I)
          SUM=SUM+DEV(I)*DEV(I)
250      CONTINUE
          RMS=SQRT(SUM/144.)
          PRINT 915,(DEV(I),I=1,144)
          PRINT 904,RMS
          C MAKING OF A(N,5) & B(N)
          C
          DO 300 I=1,144
          A(I,1)=1.
          A(I,2)=-(C3*X(I)/C(I))
          A(I,3)=-(C3*Y(I)/C(I))
          A(I,4)=Y(I)
          A(I,5)=X(I)
          B(I)=Z(I)-C(I)*C1+C1
300      CONTINUE
          PRINT 905,((A(I,J),J=1,5),I=1,144)
          PRINT 906,(B(I),I=1,144)
          C PRE-MULTIPLY A BY A-TRANSPOSE
          C
          DO 400 L=1,5
          DO 400 J=1,5
          DO 400 I=1,144
          AA(L,J)=AA(L,J)+A(I,L)*A(I,J)
400      CONTINUE
          PRINT 907,((AA(I,J),J=1,5),I=1,5)
          C PRE-MULTIPLY B BY A-TRANSPOSE
          C
          DO 500 L=1,5
          DO 500 I=1,144
          BB(L)=BB(L)+A(I,L)*B(I)
500      CONTINUE
          PRINT 908,(BB(I),I=1,5)
          C INVERT OF AA
          C CALL MINV(AA,5,D,LL,MM)
          PRINT 909,((AA(I,J),J=1,5),I=1,5)
          C SOLUTION
          C
          DO 600 L=1,5
          DO 600 I=1,5

```

75

FUXTRAN IV S	LEVEL 20		
MAIN	DATE = 77346	15/14/52	PAGE 0003
0076	S(L)= S(L)+AA(L,I)*BB(I)		
0077	600 CONTINUE		
0078	PRINT 910,(S(I),I=1,5)		
0079	C NEW Z OR BEST FITTED Z		
0080	DO 700 I=1,144		
0081	XA=X(I)-S(2)		
0082	YA=Y(I)-S(3)		
0083	ZBF(I)=C1*(SQRT(1.+(XA*XA+YA*YA)/C2)-1.)*S(1)+Y(I)*S(4)		
0084	X +X(I)*S(5)		
0085	700 CONTINUE		
0086	PRINT 911,(ZBF(I),I=1,144)		
0087	C DEVIATION FROM THE BEST FIT		
0088	C SUM=0.		
0089	DO 800 I=1,144		
0090	DEV(I)=ZBF(I)-Z(I)		
0091	SUM=SUM+DEV(I)*DEV(I)		
0092	RMS=SQRT(SUM/144.)		
0093	PRINT 912,(DEV(I),I=1,144)		
0094	800 CONTINUE		
0095	PRINT 913,RMS		
0096	DO 850 I=1,144		
0097	X(I)=X(I)/25.4		
0098	Y(I)=Y(I)/25.4		
0099	DEV(I)=DEV(I)*1000./25.4		
0100	850 PUNCH 918,X(I),Y(I),DEV(I)		
0101	850 CONTINUE		
0102	C FORMATS		
0103	C 900 FORMAT(72A1)		
0104	901 FORMAT(6F10.4)		
0105	902 FORMAT(9.9/9.9)	X Y AND MEASURED Z 9,/,,(15.3F10.4))	
0106	903 FORMAT(9.9/9.9)	PARALLEL SHIFT = 9F10.4, MM 9)	
0107	904 FORMAT(9.9/9.9)	RMS BEST-FIT BY ADJ. OF Z ONLY : 9F10.4, MM 9)	
0108	905 FORMAT(9.9/9.9)	MATRIX A 9,/,,(5F10.4)	
0109	906 FORMAT(9.9/9.9)	MATRIX B 9,/,,(10F10.4)	
0110	907 FORMAT(9.9/9.9)	MATRIX AA 9,/,,(5E15.4)	
0111	908 FORMAT(9.9/9.9)	MATRIX BB 9,/,,(5E15.4)	
0112	909 FORMAT(9.9/9.9)	MATRIX AA-INV 9,/,,(5E15.4)	
0113	910 FORMAT(9.9/9.9)	DZ = 9F10.4,	
0114	X 911 FORMAT(9.9/9.9)	DX = 9F10.4,	
0115	X 912 FORMAT(9.9/9.9)	DY = 9F10.4,	BEST-FITTED Z 9,/,,(6F10.4))
0116	X 913 FORMAT(9.9/9.9)	RX = 9E10.4,	DEVIATION FROM THE BEST FIT 9,/,,(6F10.4))
0117	X 914 FORMAT(9.9/9.9)	RY = 9E10.4,	RMS DEVIATION FROM THE BEST FIT WITH 5 DOF = 9
0118	FORMAT(2X,3F10.3)	MM 9)	